Republic of Iraq

Ministry of Higher Education and Scientific Research
University of Babylon
College of Sciences for Women
Department of Computer Sciences

Classification of Skin Cancer Images using Convolutional Neural Networks

A Thesis

Submitted to the Council of College of Science for Women, the University of Babylon in a Partial Fulfillment of the Requirements for the Degree of Master in Science\ Computer Sciences

By

Maha Ali Hussien

Supervised By

Prof.Dr.Abbas H. Hassin Al-Asadi

2023 A. D. **1445 A. H.**

بسم الله الرحمن الرحيم

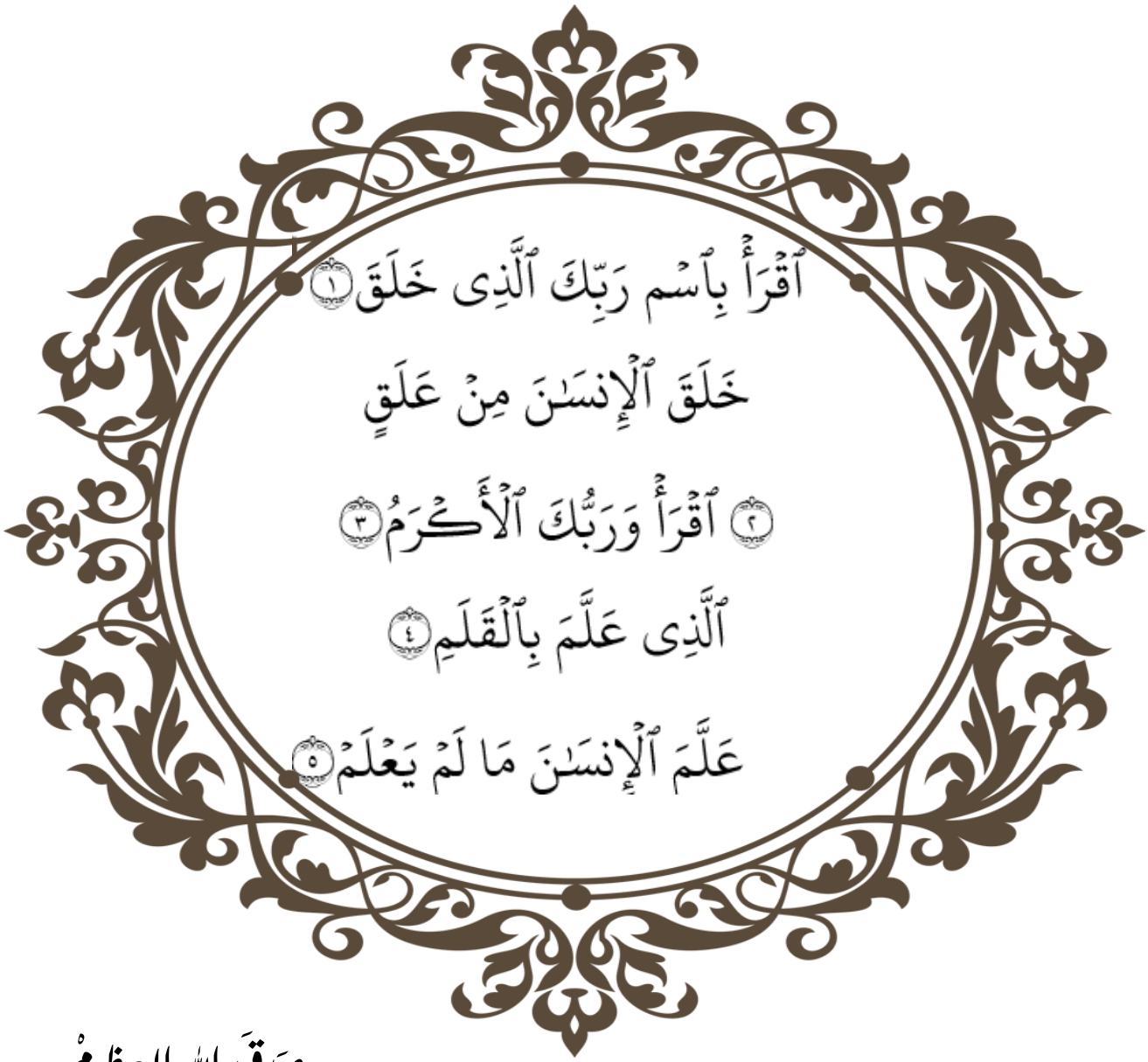

صَدَقَ الله العظِيمْ

سُورَةُ العَلَقِ الايات 1-5

Supervisor Certification

I certify that this thesis entitled

Classification of Skin Cancer Images using Convolutional Neural Networks

written by

Maha Ali Hussien

was prepared under my supervision at the College of Science for Women partial fulfillment of the requirements for the degree of a Master's in Computer Science.

Signature:

***Name: Prof. Dr.*Abbas H. Hassin Al-Asadi**

Date: / / 2023

Address:

Head of the Department Certification

In view of the available recommendations, I forward the thesis entitled "**Classification of Skin Cancer Images using Convolutional Neural Networks "** for debate by the examining committee.

Signature:
Name: Asst. Prof. Dr.saif Mahmoud Khalaf
Date: / / 2023
Address: University of Babylon/College of Science for Women

CERTIFICATION OF THE EXAMINATION COMMITTEE

We are the members of the examination committee, certify that we have read this thesis entitled (**Classification of Skin Cancer Images using Convolutional Neural Networks)** and after the examining the master student **(Maha Ali Hussien)** in its contents in 26/10/2023 and that in our opinion it is adequate as a thesis for the degree of Master in Science \ Computer Science with degree (Very Good).

Committee Chairman
Signature:

Name: **Majid Jabbar Jawad**

Scientific Order **Prof. Dr.**
Address: University of Babylon\College of Science for Women
Date: / /2023

Committee Member
Signature:
Name: **Ahmed J. Obaid**
Scientific Order: : **Assist. Prof. Dr.**
Address: University of Kufa \ Compute scienc and Mathematics .
Date: / /2023

Committee Member (Supervisor)
Signature:
'Name: **Abbas H. Hassin Al-Asadi**
Scientific Order **Prof. Dr.**
Address: University of Babylon\College of Science for Women .
Date: / /2023

Committee Member

Signature:
Name: **Ali Hadi Hassan**
Scientific Order: **Assist Prof. Dr.**
Address: University of Babylon\College of Information Technology.

Date: / /2023

Date of Examination: 26/ 10 /2023
Deanship Authentication of college of Science for Women
Approved for the College Committee of graduate studies.

Signature
Name: **Abeer Fauzi Al-Rubaye**
Scientific Order: **Prof. Dr.**
Address: **Dean of College of Science for Women**
Date: / /2023

Acknowledgments

First of all, I thank God who inspired me with patience and strength to complete this study.

It is not easy except for what God makes easy.

I would like to express my sincere thanks and appreciation to the Supervisor

"Prof.Dr.Abbas H. Hassin Al-Asadi"

To guide and follow up with me and provide important tips and suggestions to improve this study. Without him, I would not have completed this thesis. I learned a lot from him on this journey of research. I am grateful to him.

Dedication

Praise be to Allh always and forever. Praise be to Allah who we think is good and he honors us with something better than him. Thank Allh for my success in every step of my life and for passing my studies with success and excellence...Thank Allh for achieving one of the goals

To the first teacher of mankind, the prophet Mohammed, may God bless him and his family and grant them peace.

To my intercession with God in this world and the hereafter, the pure imams, peace be upon them.

To the example of dedication and devotion .... my beloved father.

To whom offered me happiness and comfort over her happiness ... My honorable mother.

To those who supported me and encouraged me with all love and patience.....my husband and daughters and son

To those who wish happiness and success for me from the bottom of their hearts without any compensation ... my dear brothers and sisters.

To all my dear loyal friends

I offer you that humble work

Maha

Abstract

Since the last two decades, melanoma skin cancer incidence rates have increased. Therefore, melanoma skin cancer has one of the highest rates of healing when caught early, quickly, and effectively. Additionally, early-stage therapy is quite simple and only requires removing the lesion from the skin. Additionally, the cost of treating melanoma skin cancer early on is fairly affordable, but as the disease progresses, it becomes more expensive due to the terrible side effects that the cancerous tumor has created. To assist physicians and patients in the diagnosis of early malignant melanoma by delivering better and more reliable results, This thesis has prasanted the method for developing a system for the detection and classification of melanoma skin cancer images in the early stage by using Convolutional Neural Networks.

In this study, the authors propose a deep-learning approach for classifying melanoma skin cancer. They introduce a convolution neural network (CNN) model that consists of 27 layers, they are skillfully created to identify characteristics in photos of skin lesions and divide them into melanoma and non-melanoma classifications. The proposed CNN model comprises multiple convolution layers that use filters to extract details like edges, forms, and patterns from the supplied image. Batch normalization layers that normalize the output of the convolution layers to accelerate the learning process and prevent overfitting follow these convolution layers. The performance of the proposed CNN model was evaluated on a publicly available dataset of skin lesion images, as well as the results demonstrated that it performed better than numerous cutting-edge approaches for classifying melanoma. The writers also carried out tests on ablation to analyze each layer's contribution to the model's overall performance. Dermatologists may be

helped by the suggested deep learning method in the early identification of melanoma skin cancer, which can lead to treatment that is more effective and improves patient outcomes. Additionally, it shows how well deep learning methods work for analyzing medical images and emphasizes the significance of properly building and improving CNN models for high performance. The accuracy of the proposed system is 99.9%.

The experimental results show that the suggested CNN model works better than current state-of-the-art methods. In summary, the proposed deep learning approach using a CNN model with 27 layers can potentially improve the accuracy and efficiency of skin lesion classification. It can be applied in clinical settings to assist dermatologists in early melanoma skin cancer detection.

List of Contents

List of Figures

List of Tables

List of Algorithms

List of Abbreviations

Abbreviations	Description
AUC	Area Under the Curve
ANN	Artificial Neural Network
BCC	Basal Cell Carcinoma
CT	computed tomography
CNN	Convolutional Neural Networks
DL	deep learning
FN	False Negative
FP	False Positive
FC	fully connected
FRCNN	region-based CNN
LMM	Lentigo Malignant Melanoma
LDA	Linear discriminant analysis
LBP	Local Binary Pattern
ML	Machine learning
MRI	magnetic resonance imaging
MSC	Melanoma Skin Cancer
NMM	Nodular Malignant Melanoma
NMSC	Non-Melanoma Skin Cancer
PCA	The principal component analysis
RGB	Color Images(Red Green Blue)
SC	Sebaceous Carcinoma
SCC	Squamous Cell Carcinoma
SSMM	Superficial spreading melanoma Malignant
SVC	Support Vector Classifier
SVM	Support Vector Machine
TN	True Negative
TP	True Positive
1D	One-Dimensional
2D	Two-Dimensional
3D	Three-Dimensional

Publications

This work has resulted in the following publication:

[1] Hussien MA, Alasadi AH. ***A Review of Skin Cancer Detection: Traditional and Deep Learning-Based Techniques***. Journal of the University of Babylon for Pure and Applied Sciences. 2023 Jun 29;31(2):253-62

[2] Maha Ali Hussien, Abbas H. Hassin Alasadi. ***Classification of Melanoma Skin Cancer using Deep Learning Approach***. TELKOMNIKA Telecommunication, Computing, Electronics and Control .

Chapter one
General Introduction

Chapter One

General Introduction

1.1 Introduction

The skin, the body's biggest organ, is critical in protecting the body from external threats such as diseases, sunburn, and wounds. The dermis, or inner layer, and the epidermis, or outer layer, are the two basic layers of skin (see Figure 1.1). [1]

Basal cells are rounded cells, whereas squamous cells are flat cells makeup epidermis. Melanocytes, pigment cells that create melanin and give the skin its natural color, are found in the lower layer of the epidermis. When sun exposure, melanocytes produce more pigment, causing the skin to darken. [1].

Important elements like lymphatic vessels, blood vessels, hair follicles, and sweat and sebum glands can be found in the dermis. The sebaceous glands keep the skin from drying out while the sweat glands assist in controlling body temperature. These glands penetrate the skin's surface through microscopic holes known na spores [1].

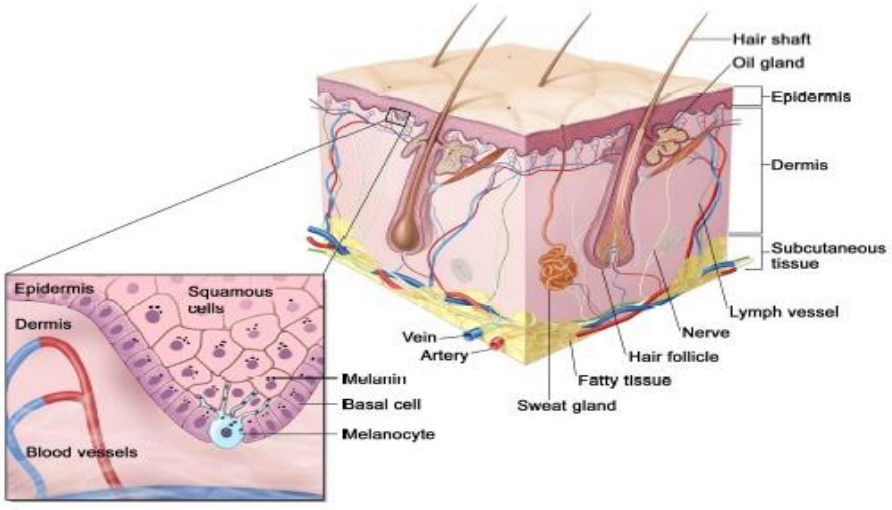

Figure (1.1): Skin Layers [1].

Skin cancer detection is a crucial area of research in computer science that involves developing algorithms and models that can accurately detect skin cancer from images of skin lesions . Traditional techniques for skin cancer detection involve manual inspection and analysis by dermatologists, which can be time-consuming and subjective.[2]

With the advancements in deep learning techniques, there has been a significant shift towards developing deep learning-based models for skin cancer detection . These models use convolutional neural networks (CNNs) to automatically learn features from the input images and make predictions about the presence of skin cancer.[3]

In recent years, several studies have compared the performance of traditional and deep learning-based techniques for skin cancer detection . These studies have shown that deep learning-based models outperform traditional techniques regarding accuracy and speed.[4]

However, some challenges are still associated with using deep learning-based models for skin cancer detection [5]. One major challenge is the need for large amounts of high-quality labeled data for training the models. Another challenge is the need for interpretability and explainability of the models to gain the trust of dermatologists and patients.

Generally, skin cancer detection is an important area of research in computer science that has the potential to improve the early detection and treatment of skin cancer significantly. Developing accurate and reliable skin cancer detection models will require continued research and collaboration between computer scientists and dermatologists

It is possible to see that the skin has two primary layers when dissecting: the epidermis, the outermost and most visible layer, and the dermis, which is

the innermost and least visible layer. The epidermis has two major parts: squamous (flat) and basal cells (round). Mesodermal melanocytes, pigment cells that create melanin, make up the lowest fraction of the epidermis. Melanin is the pigment responsible for skin color. In direct sunlight, melanocytes produce more pigment, deepening the skin's melanin and color. This layer of the skin contains lymphatic veins, blood flow, hairs, and glands. The glands in the dermis are separated into two types: those that create sweat to assist the body in regulating temperature and those that produce sebum to help prevent the skin from getting out. These glands reach the outer layer of the skin through pores, which are very small openings on the skin's surface.

Skin cancer is among the most frequent cancers. It is the main cause of death worldwide [6]. Changes in the environmental conditions we live in today have caused cancer .[7] For example, ultraviolet (UV) rays are a primary risk factor for skin cancer. In 1975, Fitzpatrick proposed a scale e from I to VI. According to the skin type and its interaction with ultraviolet (UV) rays, the first type is very light skin and is more likely to develop some skin cancer. The sixth type is dark brown, strongly pigmented skin, and less effective. herefore, this type of cancer is more common in countries with light skin. In recent decades, skin cancer incidence has climbed dramatically in the US, Europe, and Australia. Skin cancer affects one million Americans yearly, up over half of all cancers.

1.2 Related Works

The diagnosis of melanoma skin cancer is a critical aspect of early treatment and can potentially save lives. However, the current method of diagnosis, performed by trained dermatologists through visual inspection, can be subjective and prone to error. Several studies have been conducted using machine learning techniques such as Convolutional Neural Networks (CNNs) to address this issue to classify skin lesions as benign or malignant.

In 2020, Rezaoana et al. [8] .This paper suggest an automated techinic for skin cancer classification. The classification of 9 types of skin cancer has been done in this study.Also the performance and ability of deep convolutional neural networks (CNN) is observed..The dataset contains nine clinical types skin cancer ,such as -actinic keratosis,basal cell carcinoma, benign keratosis, dermatofibroma, melanoma, nevus, seborrheic keratosis, squamous cell carcinoma, vascular lesions. The objective is to establish a model that diagnoses skin cancer as well as classifies it into various classes through the Convolution Neural Network. The diagnosing methodology uses concept of image processing and deep learning.Through using different tactics of image augmentation, the number of images has also been enriched.Finally, the transfer learning approach is used to further improve the accuracy of the classification tasks.Approximately 0.76 weighted average precision, 0.78 weighted average recall , 0.76 weighted average f1-score, and 79.45 percent accuracy are shown by the proposed CNN method.

In 2021 , Junayed et al. [9] propose deep learning-based model for skin cancer detection and classification using the concept of a deep convolutional neural network (CNN). Initially, the researchers collected a dataset that included four melanoma image data before applying them in augmentation techniques to increase the size of the accumulated dataset. Next, they designed a deep CNN model to train their dataset. In the test data, their model obtained

an accuracy of 95.98%, which is better than the pre-training models, GoogleNet at 1.76% and MobileNet at 1.12%, respectively.

In 2021, Garg et al. [10] paper aims to use MNIST HAM-10,000 dataset containing dermoscopy images. The objective is to propose a system that detects skin cancer and classifies it in different classes by using the convolution neural network. The diagnosing methodology uses image processing and deep learning model. The dermoscopy image of skin cancer undergone various techniques to remove the noise and picture resolution. The image count is also increased by using various image augmentation techniques. In the end, the transfer learning method is used to increase the classification accuracy of the images further. this CNN model gave a weighted average precision of 0.88, a weighted recall average of 0.74, and a weighted F1 score of 0.77. The transfer learning approach applied using ResNet model yielded an accuracy of 90.51%.

In 2022, Aljohani et al. [11] .In this study, considered the detection of melanoma through deep learning based on cutaneous image processing. For this purpose, tested several convolutional neural network (CNN) architectures, including DenseNet201, MobileNetV2, ResNet50V2, ResNet152V2, Xception, VGG16, VGG19, and GoogleNet, and evaluated the associated deep learning models on graphical processing units (GPUs). A dataset consisting of 7146 images was processed using these models, and compared the obtained results. The experimental results showed that GoogleNet can obtain the highest performance accuracy on both the training and test sets (74.91% and 76.08%, respectively).

In 2022, Ali et al. [12]. in this study a developed a preprocessing image pipeline for this work. removed hairs from the images, augmented the dataset, and resized the imageries to meet the requirements of each model. By performing transfer learning on pre-trained ImageNet weights and fine-tuning

the Convolutional Neural Networks, we trained the EfficientNets B0-B7 on the HAM10000 dataset. they evaluated the performance of all EfficientNet variants on this imbalanced multiclass classification task using metrics such as Precision, Recall, Accuracy, F1 Score, and Confusion Matrices to determine the effect of transfer learning with fine-tuning. This article presents the classification scores for each class as Confusion Matrices for all eight models. best model, the EfficientNet B4, achieved an F1 Score of 87 percent and a Top-1 Accuracy of 87.91 percent.

In 2022, Fraiwan et al. [13] In this research, the deep learning method convolution neural network (CNN) was used to detect the two primary types of tumors, malignant and benign, c tumors. Using ESRGAN, the photos were first retouched and improved. The photos were augmented, normalized, and resized during the preprocessing step.Skin lesion photos could be classified using a CNN method based on an aggregate of results obtained after many repetitions. Then, multiple transfer learning models, such as Resnet50, InceptionV3, and Inception Resnet, were used for fine-tuning. In addition to experimenting with several models (the designed CNN, Resnet50, InceptionV3, and Inception Resnet), this study's innovation and contribution are the use of ESRGAN as a preprocessing step. designed model showed results comparable to the pretrained model. An 83.2% accuracy rate was achieved by the CNN, in comparison to the Resnet50 (83.7%), InceptionV3 (85.8%), and Inception Resnet (84%) models.

In 2023, Tahir et al. [14] they proposed a deep learning-based skin cancer classification network (DSCC_Net) that is based on a convolutional neural network (CNN), and evaluated it on three publicly available benchmark datasets . For the skin cancer diagnosis, the classification performance of the proposed DSCC_Net model is compared with six baseline deep networks, including ResNet-152, Vgg-16, Vgg-19, Inception-V3, EfficientNet-B0, and

MobileNet. In addition, used SMOTE Tomek to handle the minority classes issue that exists in this dataset. The proposed DSCC_Net obtained a 99.43% AUC, along with a 94.17%, accuracy, a recall of 93.76%, a precision of 94.28%, and an F1-score of 93.93% in categorizing the four distinct types of skin cancer diseases. The rates of accuracy for ResNet-152, Vgg-19, MobileNet, Vgg-16, EfficientNet-B0, and Inception-V3 are 89.32%, 91.68%, 92.51%, 91.12%, 89.46% and 91.82%, respectively.

In 2023, Keerthana et al. [15] This article presents two novel hybrid CNN models with an SVM classifier at the output layer for classifying dermoscopy images into either benign or melanoma lesions. The features extracted by the first CNN and second CNN models are concatenated and fed to the SVM classifier for classification. The labels obtained from an expert dermatologist are used as a reference to evaluate the performance of the proposed model. The proposed models displayed better results over the state-of-the-art CNN models on the publicly available ISBI 2016 dataset. The proposed models achieved 88.02% and 87.43% accuracy, which remain higher than the traditional CNN models.

Table (1.1) Summary of the Literature Review.

References	Dataset	Model	Accuracy%
N. Rezaoana et al. In 2020, [8]	International Skin Imaging Collaboration (ISIC)	VGG16	79.45%
M.S. Junayed et al. In 2021 , [9]	International Skin Imaging Collaboration (ISIC)	CNN	95.98%
R. Garg et al. In 2021, [10]	MNIST HAM-10,000	VGG16	90.51%
K. Aljohani et al. In 2022, [11]	ISIC 2018	ResNet50V2 VGG19	74.91%,76.08%
K. Ali et al. In 2022, [12]	HAM-10,000	EfficientNet	87.91%
M. Fraiwan et al. In 2022, [13]	DermNet NZ dataset	Resnet50	83.2%
M. Tahir et al. In 2023, [14]	ISIC 2018	CNN	99.43%
D. Keerthana et al. In 2023, [15]	ISBI 2016	CNN	88.02%

In conclusion, various studies have shown that machine learning techniques, particularly CNNs, can improve the accuracy of melanoma skin cancer diagnosis.

1.3 Problem Stentmat

Melanoma skin cancer is dangerous and potentially life-threatening, and early detection is critical for effective treatment. Currently, the diagnosis of melanoma is primarily performed by trained dermatologists through visual inspection.

To address this challenge, there is a need for a more objective and reliable method for diagnosing melanoma skin cancer. One promising approach is using deep learning algorithms, which can analyze images of skin lesions and distinguish between benign and malignant cases based on features.

1.4 Thesis Objective

This thesis aims to develop a deep learning-based system for automatically classifying melanoma skin cancer using a lightweight and efficient Convolutional Neural Network (CNN). This system should be able to accurately distinguish between benign and malignant skin lesions and provide a probability score for each class.

This thesis involves collecting and annotating a large dataset of skin images, fine-tuning a pre-trained CNN network, and evaluating the network's performance on a validation set of images.

1.4 Outline of Thesis

The following five chapters make up this thesis:

Chapter 1 The research work's thesis topic is introduced in Chapter 1, along with other pertinent information.

Chapter 2 briefly overviews the theoretical background techniques used to detect early melanoma skin cancer.

Chapter 3 discusses the steps used in the melanoma skin cancer detection system.

Chapter 4 gives the performance evaluation and experimental results.

Chapter 5 concludes the whole thesis with a short discussion, stating the problems with the tested algorithms and some suggestions for future research directions.

Chapter Two
Theoretical Background

Chapter Two

Theoretical Background

2.1 Introduction

The theoretical underpinning for using CNN is presented in this chapter. a lightweight deep neural network architecture, to classify melanoma skin cancer. Mobilenet was designed to address the limitations of traditional deep neural networks, such as high computational requirements, and has shown promising results in image classification tasks. The chapter will overview deep learning and convolutional neural networks and its key features. The potential benefits and limitations of using CNN for automated melanoma detection and diagnosis will also be discussed.

2.2 Skin Cancer

skin cancer is the most frequent kind of cancer, and its prevalence has recently increased in the United States, Europe, and Australia. With over one million diagnoses in the United States each year, it accounts for more than over 50 percent of all cancers found and one-fourth of all newly discovered malignancies. Those with lighter skin are particularly susceptible to skin cancer, characterized by the uncontrolled growth of skin cells that can invade and multiply in other parts of the body, resulting in a lesion. [16]

Skin cancer, like many other cancers, can be fatal if it is not identified and treated when it is still in the early stages [17]. Skin cancer often starts as precancerous lesions, which are not cancerous initially but can develop into malignancies over time. Thus, monitoring and treating any suspicious skin changes is crucial to prevnt skin cancer progression.

Non-Melanoma Skin Cancer (NMSC) and Melanoma Skin Cancer (MSC) are the two basic categories into which skin malignancies can be divided. About 2-3 million people are affected each year by NMSC, the most prevalent type of skin cancer. Basal Cell Carcinoma (BCC), which accounts for around 75% of all NMSC cases, and Squamous Cell Carcinoma (SCC), which accounts for roughly 24% of all NMSC cases, are the three main kinds. Additionally, roughly 1% of all cases of NMSC are sebaceous carcinoma (SC). [18].

MSC, on the other hand, is less typical than NMSC but is also more severe and aggressive. There are benign and malignant varieties of it. Commonly referred to as moles, benign melanoma develops on the skin as a brown, black, or tan patch. It often has a diameter of less than 6 millimeters and can be circular, oval, elevated, or flat. On the other hand, malignant melanoma is the most lethal variety of skin cancer and is a cancerous growth in a pigmented, bleedable skin lesion. “It consists of Nodular Melanoma, which accounts for approximately 75% of all MSC, Superficial Spreading Melanoma (representing about 15% of all MSC), Lentigo Melanoma (comprising about 10% of all MSC), and Acral Melanoma (constituting about 5% of all MSC)” [19].

It is worth mentioning that both MSC and NMSC are rare in children [18]. (see Figure 1.2).

Early diagnosis is crucial to reducing the death rate from malignant skin cancer. The treatment plan is tailored to the type of cancer, the patient's age, location, and whether it is a first occurrence or a recurrence. Effective and prompt treatment is essential for the best possible outcome and improved survival rates.

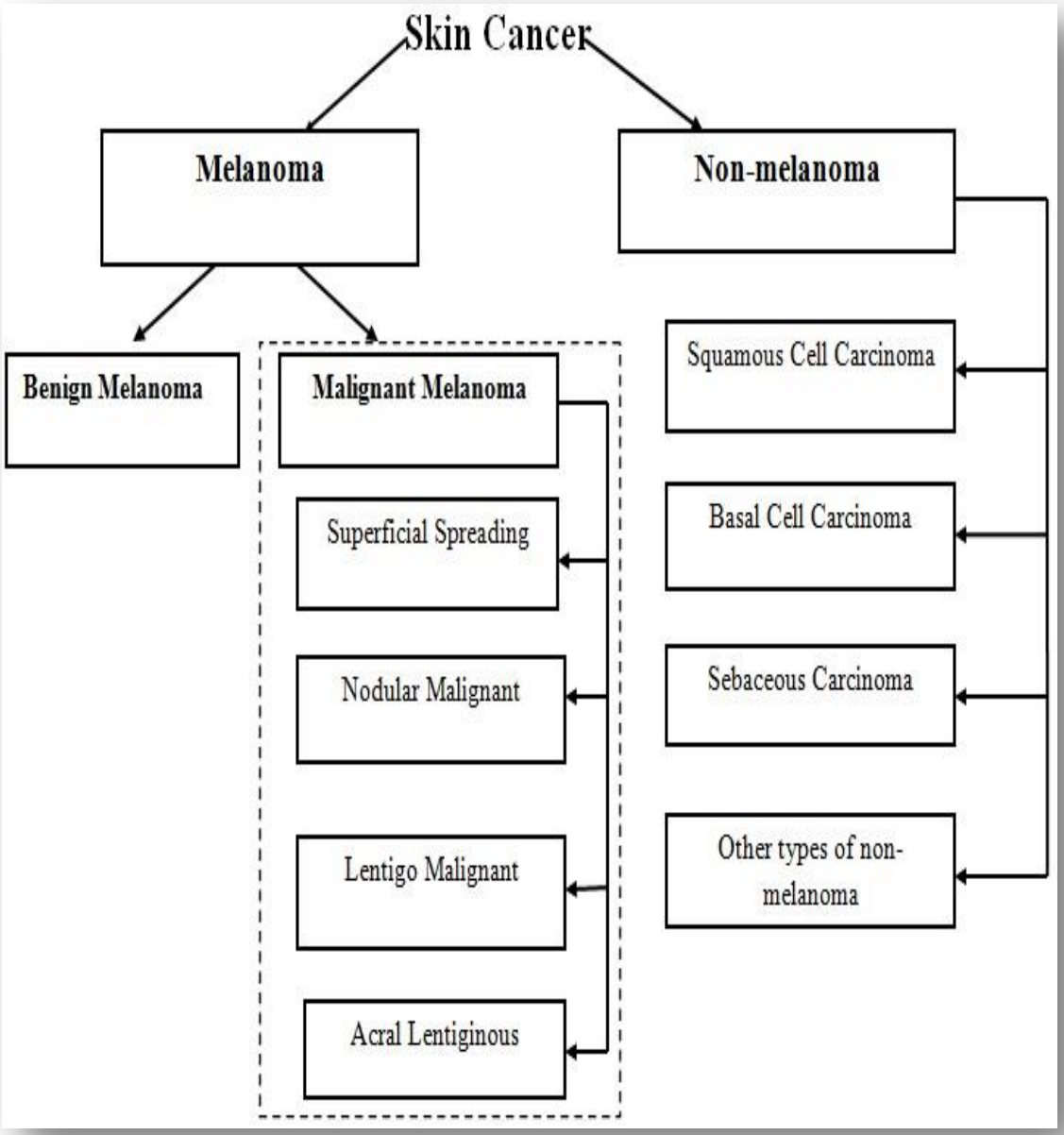

Figure (2.1): Skin Cancer Types.[18]

2.2.1 Benign Melanoma Skin Cancer

Benign melanomas develop from various skin cells, and most individuals have several moles or nevi **[20]**. While most moles are harmless, having multiple moles can increase the risk of developing malignant melanoma from benign properties. Benign melanomas can be identified by their small diameter (less than 6 mm), symmetrical shape (the shape on one side is similar to the other side), and regular border (round). Some common types of benign skin lesions include:

1. **A Spitz nevus** is a mole resembling malignant melanoma but is generally benign and non-invasive. This type is commonly seen in children, teenagers, and sometimes adults.
2. **Hemangiomas** are the growth of blood vessels, sometimes called port wine stains, strawberry spots, or cherry. This type of lesion is generally benign.
3. **Seborrheic keratoses** are brown or black spots with a waxy texture.
4. **Warts** are raised growths on the skin caused by a viral infection. They have a rough texture and can appear anywhere on the body.
5. **Lipomas** are soft growths that consist of fat cells.

The majority of these lesions scarcely turn into malignant melanoma cancers. There are many other types of benign skin lesions, but most are not widespread. Figure (1.3) shows an example of a benign melanoma skin lesion.

Figure (2.2): Benign Skin Lesions.[20]

2.2.2 Malignant Melanoma Skin Cancer

Malignant melanoma is a serious and aggressive form of skin cancer that begins in the melanocytes and can spread to bones and organs. Skin cancer is most prevalent in Australia. Though less prevalent, this type of skin cancer is more fatal than other skin cancer types. Melanoma lesions are commonly brown or black, but some cells stop producing melanin and appear pink, tan, or white. It is commonly found on women's legs, men's backs and chests, and women's faces, necks, mouths, eyes, and genitalia. Signs of malignant melanoma include large pigmented moles with a diameter greater than 6mm, asymmetric lesion shape, irregular borders, coloration, itching, and bleeding [21][22].

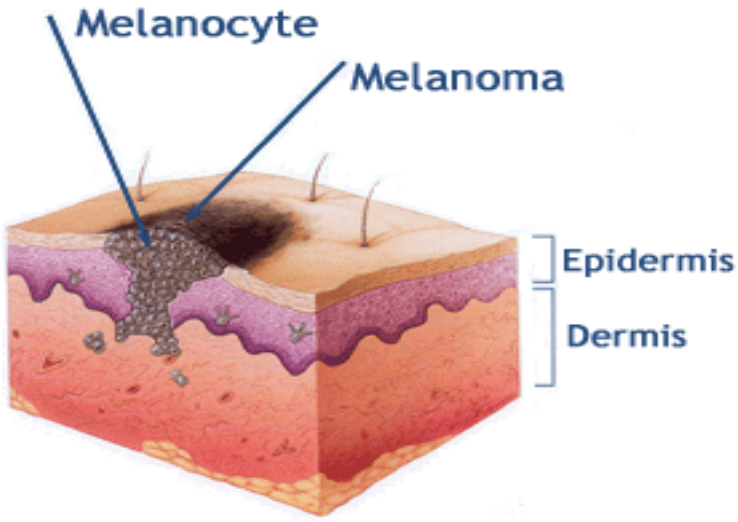

Figure (2.3): Melanoma Skin Cancer [23].

Malignant Melanoma Types **:** Malignant melanoma or called cutaneous melanoma contains four kinds which are classified by their histologic features and are listed according to their frequency of occurrence[24]:

2.2.2.1 Superficial Spreading Malignant Melanoma

Superficial spreading melanoma (SSMM) is a common type of malignant melanoma affecting people of all ages. It usually presents on women's legs, and men's trunks are larger than 0.5cm in diameter, elevated, and spread horizontally. SSMM appears asymmetrical with color variations and irregular borders and grows over months to years (radial growth), allowing for early detection when thin. Figure (1.6) shows an example of SSMM with irregular borders and variable pigmentation [24].

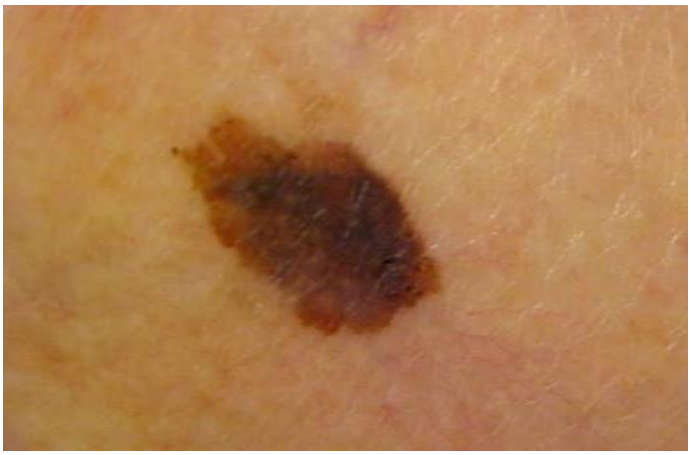

Figure (2.4): Superficial Spreading Malignant Melanoma.[24]

2.2.2.2 Nodular Malignant Melanoma

Nodular malignant melanoma (NMM) is a less common but more aggressive form of skin cancer, appearing as a dark brown or black, dome-shaped lump that bleeds and ulcerates. NMM is often thicker at diagnosis due to rapid, vertical growth from the outset, leading to a higher mortality rate. The lesion may have an irregular outline and color but often has a well-defined border and symmetry. Figure (1.7) provides an example of NMM [25].

Figure (2.5): Nodular Malignant Melanoma.[25]

2.2.2.3 Lentigo Malignant Melanoma

Lentigo Malignant Melanoma (LMM) is a type of malignant melanoma that develops in sun-exposed areas, particularly on the face of the elderly, with a mixture of pink, gray, blue, and white pigmentation. The borders are often irregular and notched. It can grow from 1.0 to 20.0 cm or larger and thickens over time, forming nodules. LMM starts as a tan macule and gradually darkens to a palpable papule, nodule, or plaque. Figure (1.8) shows an example of LMM [26].

Figure (2.6): Lentigo Malignant Melanoma.[26]

2.2.2.4 Acral Malignant Melanoma

Acral and nail melanoma is a rare malignancy on acral areas or mucous membranes. It starts as a flat, irregular lesion that becomes raised and nodular. It has limited color variations but may have irregular, notched borders and range in size from 0.9 to 12cm or more. Advanced cases show raised, blue, black, or amelanotic papules or nodules that may ulcerate. Nail melanoma affects the great toe and produces a pigmented streak in the nail plate. An example is seen in Figure (2.7) [25].

Figure (2.7): Acral Lentiginous Malignant Melanoma.

2.2.3 Non-Melanoma Skin Cancer

The most prevalent form of skin cancer is non-melanoma skin cancer (NMSC), which occurs more frequently than all other cancers combined. NMSC has poor spreadability and skin cell origins, making early detection challenging. The three subtypes of NMSC are sebaceous carcinoma (SC), squamous cell carcinoma (SCC), and basal cell carcinoma (BCC) [27].

2.2.3.1 Basal Cell Carcinoma (BCC)

A kind of skin cancer that develops from basal cells is called basal cell carcinoma (BCC) keratinocytes. the epidermis's thickest layer. Sun exposure is the cause of radiation therapy and develops slowly without spreading to other body parts. It commonly appears as a pearly white bump with translucent edges, a raised pink color, also tiny, discernible blood vessels. BCC can sometimes take the form of a mole with a pearly border. Another type has a waxy look and is flat and crusty and has an unclear boundary. Figure (1.4a) shows an example of BCC [1].

2.2.3.2 Squamous Cell Carcinoma (SCC)

Skin cancer called squamous cell carcinoma develops in the keratinocytes of the epidermis. It is caused by factors such as sun exposure, x-ray exposure, chemical damage, or skin that has been burned. It is commonly found in areas of chronic inflammation on the lips and mucous membranes. Although SCC rarely spreads, it is more likely to do so than BCC. An example of SCC is shown in (Figure 1.4b) [16].

2.2.3.3 Sebaceous Gland Carcinoma (SGC)

A sebaceous Gland carcinoma is a rare form of non-melanoma skin cancer that grows in areas of the body with sebaceous glands, such as the eyes, neck, face, leg, torso, arm, ear, mouth, genitals, and big toe [27]. It can be seen in Figure (2.8c).

(a) **(b)** **(c)**

Figure (2.8): Types of non-melanoma skin cancer [1] (a) Basal cell carcinoma (b) Squamous cell carcinoma (c) Sebaceous gland carcinoma

2.3 Digital Image

Digital images are a fundamental component of modern healthcare, providing clinicians with detailed visual information to assist in diagnosing, treating, and monitoring patients. Medical digital images can be broadly categorized into 2D and 3D. 2D images are static images that capture organs, tissues, and other structures in the body. In contrast, 3D images provide a more comprehensive view of the anatomical structures, enabling a detailed visualization of the spatial relationships between structures [28].

Medical digital images are represented in different formats, each with advantages and limitations. The most common formats used in medical imaging are raster and vector graphics [29]. Raster images, or bitmap images, are represented as a grid of pixels. Each pixel contains a numerical value that represents the brightness or color of that pixel. Raster images are suitable for capturing detailed images with complex color or texture information, but they can be vulnerable to image degradation and loss of detail when scaled or manipulated.

In contrast, vector graphics are represented using mathematical equations to describe the shape and geometry of the image. Vector images are infinitely scalable and can be resized without losing detail, making them ideal for medical imaging applications requiring high Precision and accuracy. However, vector images are less suited for capturing complex color and texture information and may require specialized software to view and manipulate [30].

In medical imaging, the choice of image format is often dictated by the imaging modality used, such as X-ray, computed tomography (CT), magnetic resonance imaging (MRI), or ultrasound. Each imaging modality has its strengths and limitations, and the choice of modality depends on the specific diagnostic question and patient characteristics. For example, X-ray imaging is commonly

used to assess bone fractures and joint abnormalities. At the same time, CT is well suited for identifying abnormalities in soft tissue structures such as the brain, chest, and abdomen. MRI is often used to evaluate the brain, spine, and joints, while ultrasound is commonly used to image the fetus and other soft tissue structures [31][32].

Moreover, deep learning and other machine learning techniques have shown promise in improving the accuracy and efficiency of medical image analysis. For example, Convolutional Neural Networks have been used to classify skin lesions in dermoscopy images, detect lung nodules in CT images, and identify breast cancer in mammography images [33].

2.3.1 Digital Image Representation

Digital images can be represented in various ways, depending on the application and requirements [28]. The most common representations include the following [29][30]:

1. ***Binary Images***: Binary images are black-and-white images where each pixel is either black (represented by a 0) or white (represented by a 1). These images are commonly used in image segmentation and object recognition.
2. ***Gray-scale Images***: Gray-scale images are composed of shades of gray, ranging from black to white. A single value represents each pixel in a gray-scale image, typically ranging from 0 (black) to 255 (white).
3. ***Color Images***: Color images comprise three or more color channels, typically red, green, and blue (RGB). Each pixel in a color image is represented by a combination of values for each color channel. In this proposed system, these images are used to diagnose skin cancer and can provide detailed information on the cancerous cells' size, depth, and invasion.

2.3.2 Image Preprocessing Steps

Image preprocessing is an essential step in medical image analysis, as it can significantly improve the accuracy and reliability of the analysis. The following are some of the commonly used image-preprocessing steps in medical imaging:

1. ***Convert RGB to Grayscale image***: In certain applications, it is necessary to convert a color image to a grayscale representation, and most of the display and image-capture technology currently on the market can only handle 8-bit images. Grayscale photographs are also more versatile and easier to process than color images, which eliminates the need to employ them for many activities. [32]. To transform a picture from RGB mode to greyscale, an equation is necessary (2.1).

$$GRAY = 0.30\ R + 0.59\ G + 0.11\ B \quad \text{... (2.1)}$$

Where: R(Red Color),G(Green Color),B(Blue Color)

2. ***Image resizing*** is a common image preprocessing step in medical image analysis that involves changing the size or resolution of the image. Resizing can be useful in various scenarios, such as reducing the computational cost of subsequent analysis steps or standardizing the size of images from different sources [34]. In skin cancer diagnosis, image resizing can be particularly useful for analyzing dermoscopic images, which can have a wide range of sizes and resolutions depending on the imaging device used. Resizing these images to a standardized size or resolution can help to improve the accuracy and consistency of subsequent analysis steps, such as segmentation or feature extraction.
3. ***Image normalization*** is particularly important in skin cancer diagnosis as it can help to reduce the impact of lighting and contrast variations on the

appearance of the lesion [35]. Normalization can be particularly useful when analyzing dermoscopic images, which can be affected by factors such as the angle of illumination and the patient's skin tone. Normalizing the pixel values to a standardized scale can minimize these variations, allowing for more accurate and consistent image analysis.

4. ***Image filtering*** removes noise and artifacts from the image, which can interfere with the analysis and interpretation of the image. Filtering techniques such as median or Gaussian filtering can smooth the image and reduce the impact of random pixel-vision variations. Filtering can help improve the image's quality and make it easier to identify important features or structures within the image, as shown in Equation (2.2) [33].

$$G(x,y) = \frac{1}{2\pi\sigma^2} e^{-\frac{x^2+y^2}{2\sigma^2}} \quad \ldots(2.2)$$

2.3.3 Digital Image Enhancement

Image enhancement is the processing of an image to enhance certain features of an image. Image enhancement improves the capacity of information in images to be interpreted or perceived by human viewers, as well as better input for other automated image processing approaches. The main goal of image enhancement is to change an image's characteristics so that they are better suited to a certain purpose and viewer. One or more picture characteristics are changed throughout this operation. A provided task determines the attributes to be used and how they are updated. The following scenarios involve the use of image enhancement: removing the image's noise The dark image is improved, and the edges of the objects are highlighted, giving the image a smoother appearance. The outcome is better suited to particular uses than the original image [34].

Enhancing images is a crucial process in various fields, involving using T to transform an image f into an image g, with r and s representing pixel values.There are various methods to enhance images, but the problem is poorly defined due to the lack of a quantifiable benchmark for image quality. Grey-level slicing, the spatial domain equivalent of band-pass filtering, can highlight certain intensities while underplaying others or highlight certain grey levels while ignoring others.

Histograms normalize images using histogram processing technique, enhancing them by reducing pixel count. It is a discrete function for a digital image's histogram to have intensity levels between [0, L-1]. To increase the intensity of photographs, the histogram enhancement approach is performed [35].

The resulting image's histogram is systematically flattened and stretched using the spatial domain technique known as histogram equalization. It generates an image with a consistent distribution of pixel intensity as the result. This straightforward, effective method is commonly used for image-enhancing paradigms [36].

Histogram equalization enhances contrast in various applications, such as radar signal processing and medical picture processing, due to its simplicity and effectiveness. The brightness of a picture can fluctuate after histogram equalization, primarily because of the histogram equalization's flattening property. This is one disadvantage of histogram equalization. This technique generally expanded the overall contrast of multi-images, particularly when an adjacent contrast value illustrates the applicable data of the image.

The modification achieves that the intensities distribution could be finer on the histogram, It makes it acceptable for locations with poor local contrast to have a good contrast. Histogram equalization is accomplished by effectively dilating the

most frequent intensity values [37]. According to Equation (2.3), the histogram cumulative distribution function is crucial for computing histogram equalization.

$$Cdf\,(X) = \sum_{i=1}^{x} h(i) \qquad \ldots(2.3)$$

The gray value is represented by X, and the histogram of the image is shown by h.

$$T[pixel] = round\,\left(\left(\frac{cdf(x) - cdf(x)_{min}}{E*F - cdf(x)_{min}}\right) * (L - 1)\right) \qquad \ldots (2.4)$$

$cdf(x)_{min}$:- The cumulative distribution function's minimal value.

E * F:- Number of picture rows and columns

L:- 256 gray levels were employed.

2.4 Feature Extraction Approaches

Feature extraction is a method used in pattern recognition and image processing to extract crucial information from original data and represent it in lower-dimensional space. This technique is used when input data is too large and redundant, transforming it into a reduced representation set of features, also known as a features vector. This dimensionality reduction helps in the easier classification of patterns.

Feature extraction transforms input data into a set of features that extract information for tasks using condensed representations. Pattern recognition is a relatively new area of image processing research that is utilized in a variety of applications including data input, character recognition, document verification, bank deposit slips, checks, credit card applications, check sorting, face and script recognition, and postal address reading [38].

Feature extraction is done after the preprocessing phase in the system. An effective feature set comprises discriminating data that sets one thing apart from another. Features can be divided into two categories, and they must be as resilient as possible to prevent producing different feature codes for objects belonging to the same class [39] :

1. Local aspects, such as concave and convex sections, the number of endpoints, branches, joints, etc., are often geometric.

2. Global features are typically topological or statistical (invariant moments, etc.), including connectedness, projection profiles, and the number of holes.

Focusing on the feature extraction stage is crucial since it affects the detection system's effectiveness measurably.

2.4.1 Linear Discriminant Analysis

Linear Discriminant Analysis (LDA) is a popular supervised scheme commonly employed in computer vision to reduce dimensionality. This classical statistical method decreases dimensionality while preserving class-specific information. It is a strong yet straightforward methodology suitable for various applications. LDA computes the feature space by determining the eigendecomposition of a suitable matrix, assuming data is provided in advance. However, in cases where data is provided sequentially, gradual updating of LDA characteristics is necessary through observation of incoming samples [40].

For the LDA approach to be used as intended, all samples must be submitted in advance. The data input is, however, sometimes seen as a stream when the whole data set is unavailable. Without repeating the process on the whole set of data,

LDA feature extraction in this scenario ought to be able to update the computed LDA features by watching the new samples.

LDA techniques are used in various research areas, such as bioinformatics, text recognition, and facial recognition. They compress high-dimensional feature vectors into lower-dimensional spaces, allowing easy separation of one class's vectors from others [41].

2.4.2 Local Binary Pattern (LBP)

A potent technique for texture description is the original Local Binary Pattern (LBP) operator, which was first presented by Ojala et al. [42]. By thresholding each pixel's 3x3 neighborhood with its center value and treating the result as a binary number, the operator identifies the pixels in a picture [43].

Two expansions were developed for the original operator, acquiring strong features in circular neighborhoods. Bi-linear interpolation recognizes pixel numbers and radius, resulting in a representation of geographically separated P sample points on a circle.

The proposed characterizing image textures using 2p subsets and the LBP operator for local binary patterns. The uniform local binary pattern [44] is the name of this pattern's smaller subset. The number of bitwise shifts from 1 to 0 or vice versa makes up the pattern. If the LBP's uniformity measure is at most 2, it is considered uniform.

2.4.3 Principle Component Analysis

Technical statistic known as the principle component analysis (PCA) transforms a set of observations of potentially correlated variables into values of linearly uncorrelated variables via an orthogonal transformation. PCA is an effective feature extraction method in this field [45]. The goal is to describe patterns with fewer features and reduce feature space dimensionality without losing crucial detection information.

Principal Component Analysis (PCA), also known as Karhunen-Loeve expansion, is a classical technique for feature extraction and data representation in computer vision, focusing on essential features [46] [47],

The unsupervised algorithm uses a linear transformation method that finds the largest variance in the data to create new features. When analyzing a large dataset, PCA reduces the number of possible dimensions by projecting the data onto a smaller number of orthogonal axes. The variance of the first PC is greatest during the transformation, while the variances of the succeeding PCs are progressively smaller. PCA method first constructs the Eigenvalues of the covariance matrix, which are then transferred onto the feature space [48].

The basic idea behind principal components can be given by equations [49]:

- Compute the mean feature vector:

$$\mu = \frac{1}{p}\sum_{k=1}^{p} x_k, \qquad \ldots 2.5$$

  Where x_k pattern $(k = 1 \text{ to } p), p =$ pattern number, x feature matrix

- To get data centration, will subtract the mean from each data point.
- Compute the covariance matrix of the extracted features:

$$Cov = \frac{1}{p}\sum_{k=1}^{p}\{x_k - \mu\}\{x_k - \mu\}^T \quad \ldots 2.6$$

Where T matrix transposition.

- Compute Eigenvalues λ_i and Eigenvectors v_i of the covariance matrix:

$$Cov(v_i) = \lambda_i \, . v_i \quad \ldots 2.7$$

Where $(i = 1,2,3,\ldots q), q = \text{feature number}$

- Estimating high-valued eigenvectors and arranging all the Eigenvalues in descending order.
- A few features with high Eigenvalues will be fitting for further analysis:

$$\left(\sum_{i=1}^{s}\lambda_i\right)\left(\sum_{i=1}^{q}\lambda_i\right)^{-1} \geq \theta \quad \ldots 2.8$$

Where $s = n$ is the number of highly valued λ_i selected

- As a result, the feature matrix is simplified to a low dimension feature vector (principal components):

$$\boldsymbol{P = V^T \, . \, x} \quad \ldots 2.9$$

Where V is the matrix of principal components and x the feature matrix.

Figure (2.9) shows an example of 3D distribution as the original data points are scattered, the new ones are more compact, and noisy, and redundancy is reduced.

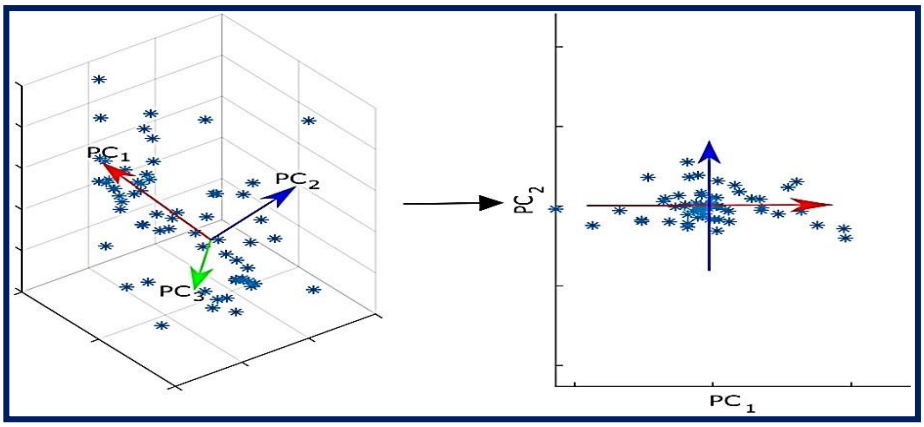

Figure (2.9): **The PCA technique for dimensionality reduction [50].**

This system chooses Principle Component Analysis to extract the features from the collected dataset.

2.5 Machine Learning

Recently, machine learning (ML) has become a more widely used technology. The internet, which generated several petabytes of data, completely changed how we live and conduct business in the 1990s and 2000s. Once the data has been transformed into predictions that can be used, machine learning and predictive analytics are once again changing our civilization. [51] .

Machine learning studies automatic techniques for learning to make accurate predictions based on past observations, and It is typically understood to include logical or binary operations-based autonomous computing methods that figure out how to do a task by studying a set of instances. The goal of machine learning is to provide classification expressions that are understandable to people. They must closely resemble human reasoning to offer an understanding of the decision-making process. Machine Learning can be defined as a process of building

computer systems that automatically improve with experience and implement a learning process [52].

The most significant application of machine learning is in data mining. People are frequently prone to making mistakes when conducting studies or even when seeking to uncover correlations between diverse variables. Because of this, they struggle to come up with solutions. These issues are frequently successfully addressed through machine learning, increasing system effectiveness and machine design as well as it can automatically extracting a piece Building effective probabilistic models that are excellent for fields with a lot the lack of a comprehensive theory of data can help extract relevant information from a body of data. The same characteristics are utilized in each instance in every dataset that machine learning techniques are applied to be represented. The traits could be continuous, categorical, or binary [53].

2.5.1 Machine Learning Algorithms

The machine learning algorithms can be divided into three primary groups: supervised, unsupervised, and semi-supervised, according to how they handle the collection of provided features and cases.

A function is taught from training data using ***supervised learning***, a machine learning technique. Pairs of desired output and input items (often vectors) make up the training data. The function's output can either be a continuous value (referred to as regression) or a classification prediction for the input item. After viewing numerous training instances, the supervised learner's objective is to forecast the function's value for each valid input item. In classification and regression, supervised learning makes use of labeled instances (X and Y) to forecast their connection [54]. All training samples must be labeled in supervised learning to produce the correct outputs.

Machine learning techniques known as ***"unsupervised learning"*** do not utilize operator input labeling. It differs from supervised learning approaches, which teach computers how to carry out tasks like utilizing a set of examples for classification or regression that humans have provided. Unsupervised learning entails that we just receive the Xs and a minimal amount of performance feedback. For tasks like clustering, compression, feature extraction, etc., the unsupervised is more difficult because cases are left unlabeled so that researchers can learn more about their distribution. Unsupervised learning has many benefits, including objectivity since the samples do not need to be categorized by specialists or data analysts. Even in the absence of prior knowledge, it can still perform effectively [55].

Recentty, ***semi-supervised learning*** has gained popularity. It is assumed that training samples with and without labels are both accessible. It is a development of labeled- and unlabeled-data-working supervised and unsupervised learning approaches. The great majority of the data, which is unlabeled, is utilized. Labeled data optimize the margin between classes, while unlabeled data determines space's geometrical structure. Semi-supervised learning is a machine learning approach that combines labeled and unlabeled data, offering advantages in various applications. It trains models using both labeled and unlabeled data, making it a valuable tool in machine learning [56]. It is possible and frequently advantageous to use information from unlabeled data to influence learning.

2.5.2 Support Vector Classifier

A supervised machine learning approach for classification tasks is called the Support Vector Classifier (SVC). SVC separates the data into two classes by mapping data points to a high-dimensional space and determining the best hyperplane [54].

SVC can be used for a linearly separable two-class learning task. It finds a hyperplane that can separate two classes of a given sample with a maximum margin, which is why it is often known as a maximal margin classifier. This margin is capable of providing the best generalization ability. Generalization refers to the fact that a classifier has a good classification performance (e.g., accuracy) and guarantees high predation [57]. Figure (2.10) depicts the optimum SVC hyperplane for a linear case.

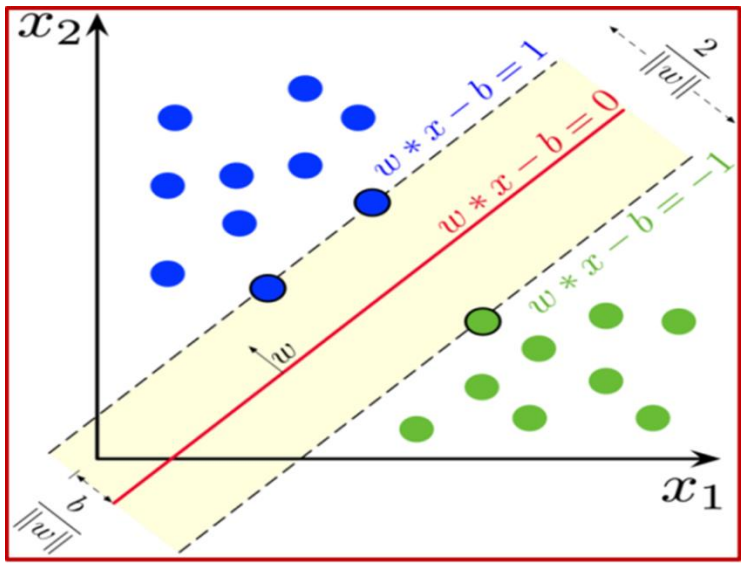

Figure (2.10): The Support Vector Machine Algorithm [57].

SVM was primarily developed to address binary classification issues, but due to its robustness, it has since been expanded to encompass regression analysis.

The SVM classifier builds hyperplanes iteratively to determine a decision boundary to divide data points into several groups. The hyperplanes are selected to maximize the distance between the decision boundary and the support vectors and to increase the proportion of training set points that are properly classified.

If a hyperplane can perfectly segregate the data, then an endless number of hyperplanes might accomplish the same thing.

2.5.3 Naïve Bayes (NB)

The naive Bayes (NB) supervised classifier is a probabilistic model that uses the joint probabilities of terms and categories to estimate the probabilities of categories. The naive Bayes learner combines Bayesian reasoning with the assumption of independence among the measurable features. It uses standard probability distribution methods to learn relative frequencies of different classes and feature values in the training data to estimate the class probability and the conditional probability distribution of a class given the feature values [58]. The beauty of the naïve Bayes approach is that the estimation of one feature distribution is completely decoupled from the estimation of others[59].Bayesian classifiers assign the most likely class to a given example described by its feature vector and has proven it efficiency in many practical applications, including text classification, medical diagnosis, and systems performance management. The Naïve Bayesian operates as follows: Given C_n classes and each one of these classes has its own probability $P(C_n)$ evaluated from the training dataset and show the prior probability of classifying an attribute V_j into $C_{n.}$ For attribute value, V_j, so the classification utilized is to find this probability is illustrated in the equation bellow:

$$\frac{P(v_1 \wedge v_2 .....v_j \mid c_n)P(c_n)}{P(v_1 \wedge v_2 .....v_j)} \quad \text{..... (2.10)}$$

2.5.4 Random Forest Classifier

Random Forests (RF) are a ML classification approach and development of a decision tree that works by constructing numerous decision trees while training the model. It is a kind of additive model that produces predictions based on a mixture of base model decisions. Decision trees have a great deal of depth and have a tendency to overfit findings. To average out the findings, RF employs numerous decision trees. A portion of the training data is used to generate a set of decision trees using the random forests classifier. It aggregates the results from different decision trees and then decides the final classification of the test data. The subsets of data used in the decision trees may overlap [60]. Figure (2.3), is an example of the process of creating multiple trees. The classification results are provided for each tree. The final categorization is based on the number of classes formed by these trees (majority class).

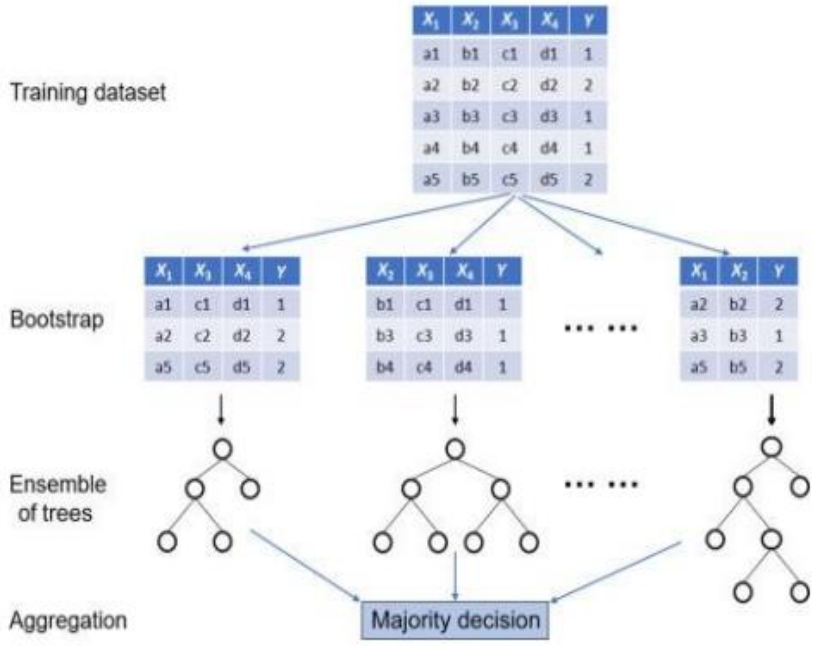

Figure (2.11): Random Forest [60]

2.5.5 Logistic Regression

It is a categorization model which is linear .It demonstrates a likelihood of a group Y set a feature-vector X. This is done via utilizing a logistic methods to discover a relation between the class and the feature-vector. It supposes the distribution P (Y|X), here Y is the class and X is the feature-vector, is on a borderline shape and after that demonstrates it from the training data. The likelihood P (Y|X) of X belongs to class Y is set by the sigmoidal function [61] .This will be explained in equation 5 and 6.

$$\mathbf{z(Y,X)} = \sum_{\boldsymbol{i=1}}^{\boldsymbol{N}} \boldsymbol{w_i f_i}\ \boldsymbol{(Y,X)} \qquad \text{…. (2.11)}$$

$$\boldsymbol{p(Y|X)} = \frac{\mathbf{1}}{\mathbf{1+\exp(-z(Y,X))}} \qquad \text{…. (2.12)}$$

Where:

P is the likelihood of (Y|X)

Y is the class

X is the feature-vector

w is the weight of the word

i is randomly chosen

exp is the exception and f is the frequency.

P (Y|X) is demonstrated via linearly linking the characteristics X multiplied with some weight w_i and performing a function $f_i\ (Y,X)$ on the relationships.f_i is a function that set a link between a characteristic of a class and a characteristic in a feature-vector in the shape of true or false on the base of the likelihood being over a certain threshold. Many characteristics are further significant than others, so the weight w_i indicates the "strength" of the characteristic [61].

LR classifier utilizes a distinctive model which implies that it can count P (A|B) immediately, with no necessity to count the probability of P (B|A) firstly. According to these distinctive features, it can be purposed that it has comparatively weak asymptotic fault in contrast to the generative manner with request more groups of training data to perform it [61].

A multi-class example of LR is the One-vs-Rest method, the classifier is trained for every group or class. It is predicted that if there is any observation to the group or class or not. After that, in order to categorize further scanning or observations, you can choose the group or class that has classifier maximizes the likelihood of the scanning or observations relating to it [62]. In figures (a), (b), and (c) of Figure (2.12) the data from every solitary group or class is suitable for their own classifiers.

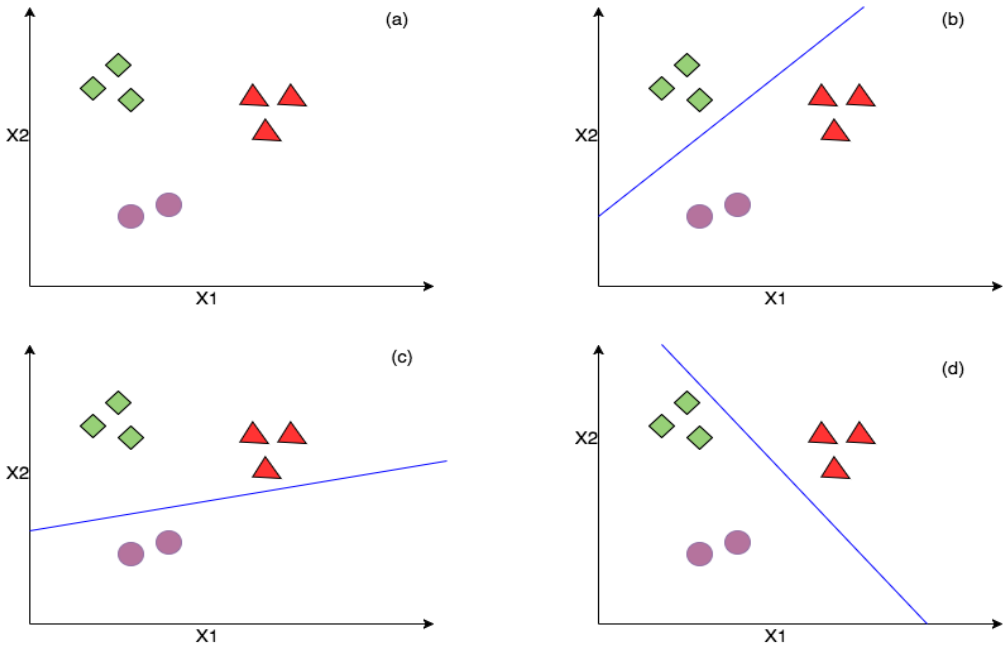

Figure (2.12) example on Logistic Regression

(a) Feature-vectors | (b) Classifier for diamonds

(c) Classifier for circles | (d) Classifier for triangles [62]

The other multi-class example of LR is to put the logistic function in equation 6 with the SoftMax function which we show in equation 5 and 7 [62].

$$\mathrm{p(y}|X)y_{\in}Y = \frac{\exp(z(y,X))}{\sum_{\acute{y}\in} y \exp(z(\acute{y},X))} \quad \ldots.(2.13)$$

Where:

p is the likelihood

x is the feature vector

Y is the set

y is the class

ŷ is the class that is produced

exp is the exception.

According to explanation in equation 7 which can be seen $\sum_{y\in Y} \mathrm{P(y}|X) = 1$, that results a classifier to a feature-vector X that produces the class yˆ when the class of the feature-vector is necessary only and not the likelihood itself [61].

$$\acute{\mathbf{y}} = \mathbf{arg}\,\boldsymbol{max}_{\boldsymbol{y}\in\boldsymbol{Y}}\,\boldsymbol{P}(\boldsymbol{y}|\boldsymbol{X}) \quad \ldots.(2.14)$$

2.6 Deep Learning

Deep learning is a machine learning technique using hierarchical layers for non-linear information processing, enabling models to learn complex representations and patterns from input data [63].

In the 1990s, the neural network community found training multi-layered networks with backpropagation and gradient-following algorithms impossible. Deeper neural networks with random initialization performed inferior to those with hidden layers [64]. Multi-layer networks have a high saddle point-local minima ratio, causing weights to grow unrestrainedly or contract to zero. The term "stacked neural networks" refers to networks with multiple layers, which is the primary distinction between the original neural network and the one used in deep learning as shown in Figure (2.13). Deep learning methodologies enable powerful tools for big data analysis, handling unlabeled data. Conventional neural networks are crucial, but other types are also utilized.

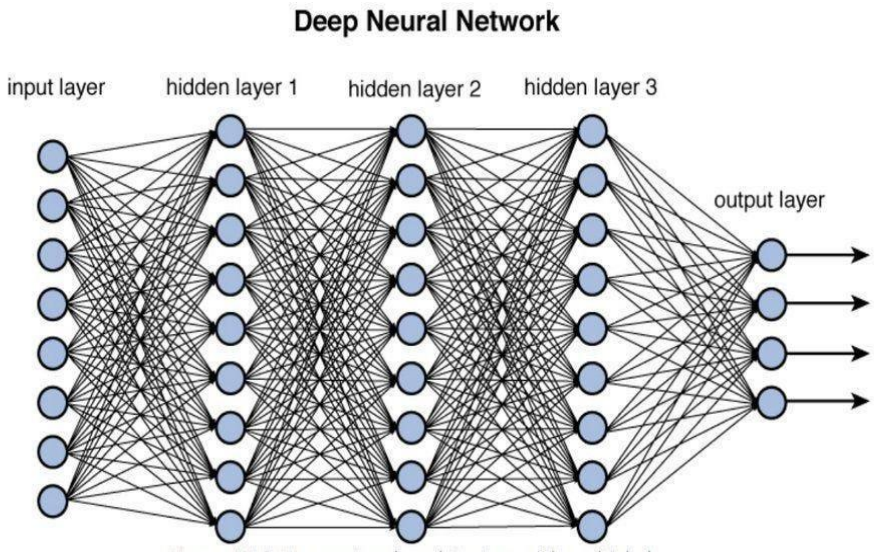

Figure(2.13): Layers of Deep Neural Networks [64]

2.6.1 Convolutional Neural Network

A subtype of the discriminative deep architecture, convolutional neural networks (CNNs) have demonstrated adequate processing efficiency for two-dimensional data having grid-like topologies, such as pictures and movies [65].

Deep 2D Convolutional Neural Networks (CNNs) are powerful tools for various technical applications involving 2D signals, such as images and video frames. Inspired by the visual cortex in the human brain, CNNs mimic the process of detecting light in distinct subregions of the visual field. By leveraging labeled data, CNNs can recognize complex visual patterns, making them suitable for tasks like image classification, object detection, and image segmentation. They automatically learn relevant features from the data, making them versatile and widely applicable.

Deep 2D CNNs have demonstrated impressive performance in various computer vision tasks, from recognizing objects in images to analyzing video frames. Research and advancements in deep learning, particularly in computer vision, continue to unlock new possibilities and applications for 2D signal processing using CNNs.

2.6.2 Architecture of CNN

The input image will pass through layers of convolution with (Kernals) filters, pooling, and categorizing using fully connected layers (FC) objects having probabilistic values ranging from 0 to 1. CNNs operate identically With one, two, or three dimensions. The input data structure and filtering, such as convolution kernels or feature detectors, significantly impact the CNN layers in this thesis.

The 1D parameters are described and demonstrated [66]:

1. ***1D convolution layer :*** 1D Convolutional Neural Networks (1D CNNs) are a modified form of 2D CNNs that require minimal computer power. With straightforward configurations and real-time implementation, 1D CNNs are affordable and feasible. They produce outputs by passing a convolution kernel across a single spatial dimension.
2. ***MaxPooling:*** A pooling layer is added after a convolutional layer applies nonlinearity, such as ReLU, to feature map output. The Max-Pooling method obtains the maximum output, increasing spatial abstractness and feature abstractness. This operation calculates the maximum value for each patch of the feature map and downsamples the input representation for 1D temporal data by taking the maximum value over the pool-size window. Strides shift the window. The resulting output, when using the "valid" padding option, has a shape of output_shape = (input_shape - pool_size + 1) / strides).
3. ***Dense Layer***: The dense layer is the standard layer in a strongly linked neural network, performing a process on input and returning the result. The number of neurons/units in the dense layer affects the output shape. The process is carried out by Dense under Equation (2.15).

$$output = activation\ (dot(input, kernel)\ plus\ bias) \quad \ldots (2.15)$$

Bias is a bias vector created by the layer, a kernel is a weights matrix, and activation is an element-wise activation function provided as input.

4. **Activation Function:** Activation functions are crucial components in neural networks that introduce non-linearity and help regulate the output of neurons, contributing to the model's ability to learn and make accurate predictions on complex datasets. ReLU is a commonly used activation function that has proven effective in deep learning architectures.. This function can be represented as shown in Equation (2.16).

$$f(x) = \max(0, x) = f(x) = \begin{cases} x, & x > 0 \\ 0, & x < 0 \end{cases} \quad \text{... (2.16)}$$

The ReLu function, with a 1 derivative for positive input, accelerates deep neural network training by enabling quick computation of error terms. It does not cause vanishing gradient issues when layers increase, and there are no asymptotic upper and lower bounds for this function.

5. ***Softmax Function***: The softmax function is a mathematical function that transforms a K-dimensional vector of real values into a K-dimensional vector of probabilities, representing a categorical distribution. It is commonly applied to the output of the final layer in neural networks, particularly in multi-class classification tasks. This conversion converts the raw numerical values assigned to each class into a probability distribution, indicating the likelihood of each class being the correct prediction. The highest probability class is considered the model's final prediction. The probabilities obtained from the softmax output can be used as input for decision-making algorithms and ensemble models, enabling integration with complex pipelines for various applications. Equation (2.17) is used to calculate the softmax function.

$$f(xi) = \frac{\exp(xi)}{\sum_{j=1}^{K} \exp(xj)} \quad \text{… (2.17)}$$

And its derivative is expressed in Equation (2.18):

$$\acute{f}(xi) = f(xi)(1 - f(xi)) \quad \text{… (2.18)}$$

Where(xi) is input vector, K is some classes in a multi-class classifier.

6. ***Stride***: Stride is a step parameter in convolutional neural networks, used to compress image and video data. It changes the amount of movement in an

image or video. If set to 1, stride moves one pixel or unit at a time. Stride is often adjusted to a whole integer, as it affects the encoded output volume.

7. ***Padding***: Padding in convolutional neural networks refers to adding extra pixels to the edges of an image to allow for more accurate analysis. The amount of padding can be adjusted; the most common type is zero padding. This process extends the area where a CNN processes an image and enables more precise feature detection.
8. ***Flatten***: the output of the preceding layers into a single vector that can serve as an input for the following layer.

Moreover, in feature extraction, CNNs are dependent on prior knowledge and human interference [66]. CNNs are used in many applications, such as Recognition of objects, voice, handwriting, faces, computer vision, handwriting analysis, behavior, and picture categorization are a few examples. Figure (2.14) depicts CNN's straightforward architecture.

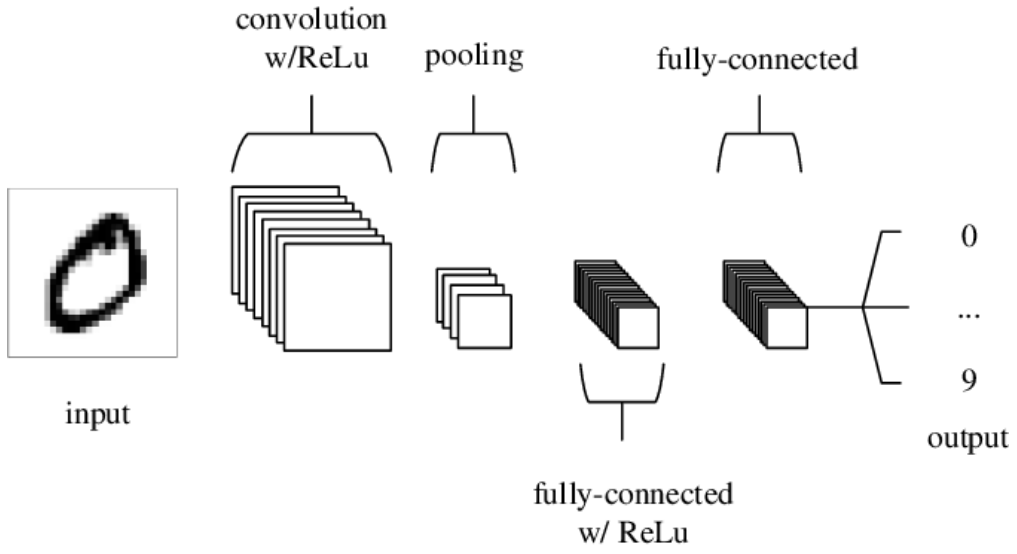

Figure (2.14): A Basic Diagram of CNN's Architecture [67].

2.6.3 MobileNet CNN

MobileNet is a TensorFlow model designed for mobile computer vision applications. It introduces depth-wise separable convolutions, reducing the number of parameters compared to traditional convolutions. This results in lightweight deep neural networks, which achieve a balance between accuracy and efficiency [68].

Google open-sourced MobileNet, which is an excellent starting point for training compact and fast classifiers, focuses on optimizing Multiply-Accumulates (MACs) to maximize accuracy while considering limited resources for on-device or embedded applications [69]. MobileNets are resource-constrained, meaning they are small in size, have low latency, and consume low power. They can be tailored to various use cases, such as image segmentation, feature embedding, object detection, and image classification.

MobileNet represents a significant advancement in creating efficient neural networks for mobile applications, enabling computer vision tasks on resource-constrained devices without compromising accuracy and performance. It is versatility and compact design has made it widely adopted in real-world applications where computational efficiency is crucial.[69]

2.7 Performance Measures

It is crucial to evaluate the machine learning model's quality to keep enhancing it until it performs as effectively as it can. Numerous real-world applications, including email spam identification, fraud detection, target marketing, and medical diagnostics, use these measures [70]. Confusion matrix, accuracy, error rate, sensitivity, specificity, etc. are all included in the evaluation of model performance.

The following parameters are used for evaluating the classifier's performance [71]:

- True positive (TP) is the accurate classification of the positive class. For example, if a model correctly isolates the cancer component of an image, including malignant cells, the resulting classification determines the existence of cancer.
- True negative (TN) is the correct categorization of the negative class; for example, the model after classification claims that no cancer is present, even if none is evident in the image.
- False positives (FP) are erroneous positive predictions; for example, the model may categorize a picture as not having cancer while it includes harmful cells.
- False negatives (FN) are inaccurate predictions; for example, a model may predict an image is malignant even when it contains no malignancy.

2.7.1 Confusion Matrix

The classification model's performance can be seen in a two-dimensional matrix called the confusion matrix, also known as the error matrix. The confusion matrix is built for binary class categorization by default. It can, however, be expanded to classify numerous classes. Table (2.1) illustrates a confusion matrix for binary class classification.

Table (2.1): Confusion Matrix Illustration for Binary-class Classification.

Confusion Matrix		Actual Class	
		Positive (p)	Negative (N)
Predicted Class	Positive (p)	True Positive (TP)	False Positive (FP)
	Negative (N)	False Negative (FN)	True Negative (TN)

The predictions made by the model are denoted by the row labels Positive and Negative. The ground-truth labels for the data set are referenced by the column labels Positive and Negative.

2.7.2 Accuracy

The proportion of correctly identified samples to all samples is known as the model accuracy. Equation (2.19) serves as a mathematical notation for it.

$$Accuracy = \frac{TP+TN}{TP+TN+FP+FN} \quad \ldots (2.19)$$

Where:

TN: is the number of true negatives.

TP: is the number of true positives.

FN: is the number of false negatives.

FP: is the number of false positives

2.7.3 Recall

A recall is the proportion of accurately predicted cases to all observed positive instances in the ground data. It displays the categorization effectiveness of occurrences with positive labels. Sensitivity or true positive rate (TPR) are other names for it. Equation (2. 20) serves as a mathematical notation for it.

$$\textbf{Recall} = \frac{TP}{TP + FN} \quad \ldots (2.\ 20)$$

Where:

TN: is the number of true negatives.

TP: is the number of true positives.

FN: is the number of false negatives.

FP: is the number of false positives

2.7.4 Precision

The ratio of correctly anticipated, actually positive events to all instances categorized as positive is known as precision. Equation (2.21) serves as a mathematical notation for it.

$$\textbf{Precision} = \frac{TP}{TP + FP} \quad \ldots (2.21)$$

Where:

TN: is the number of true negatives.

TP: is the number of true positives.

FN: is the number of false negatives.

FP: is the number of false positives

2.7.5 F1-score

Increasing one at the expense of lowering the other is a common inverse relationship between recall and precision. So, we need a statistic that strikes a balance between the two. The F1 score was developed for this purpose. The harmonic mean of recall and precision is the name of this measure. Equation (2.22) serves as a mathematical notation for it.

$$\textbf{F1-score} = 2 \times \frac{\textbf{Precision} \times \textbf{Recall}}{\textbf{Precision} + \textbf{Recall}} \quad \ldots (2.22)$$

Chapter Three

Proposed System Design

Chapter Three

Proposed System Design

3.1 Introduction

This chapter explains how the research was conducted in the thesis. It includes the algorithms and illustrations used. The methodology consists of organized steps, from collecting data to evaluating it. The main goal is to solve research problems and achieve the best results for the thesis objectives. The methods and steps proposed contribute to addressing the research problem and ensuring the best possible outcomes.

3.2 Research Methodology

In this thesis, two proposals have been put forward for analyzing skin cancer images. The first proposal suggests using traditional machine learning algorithms for feature extraction and classification. This involves applying established algorithms to extract relevant features from the skin cancer images and then using classification techniques to classify the images into different categories based on these extracted features.

The second proposal, on the other hand, involves utilizing deep learning algorithms, using Convolutional Neural Networks

It is important to note that both proposals incorporate a preprocessing stage. This preprocessing stage is a crucial step in the overall image analysis process and involves a series of steps before the images' actual processing. The proposed algorithm's block diagram is displayed in Figure (3.1).

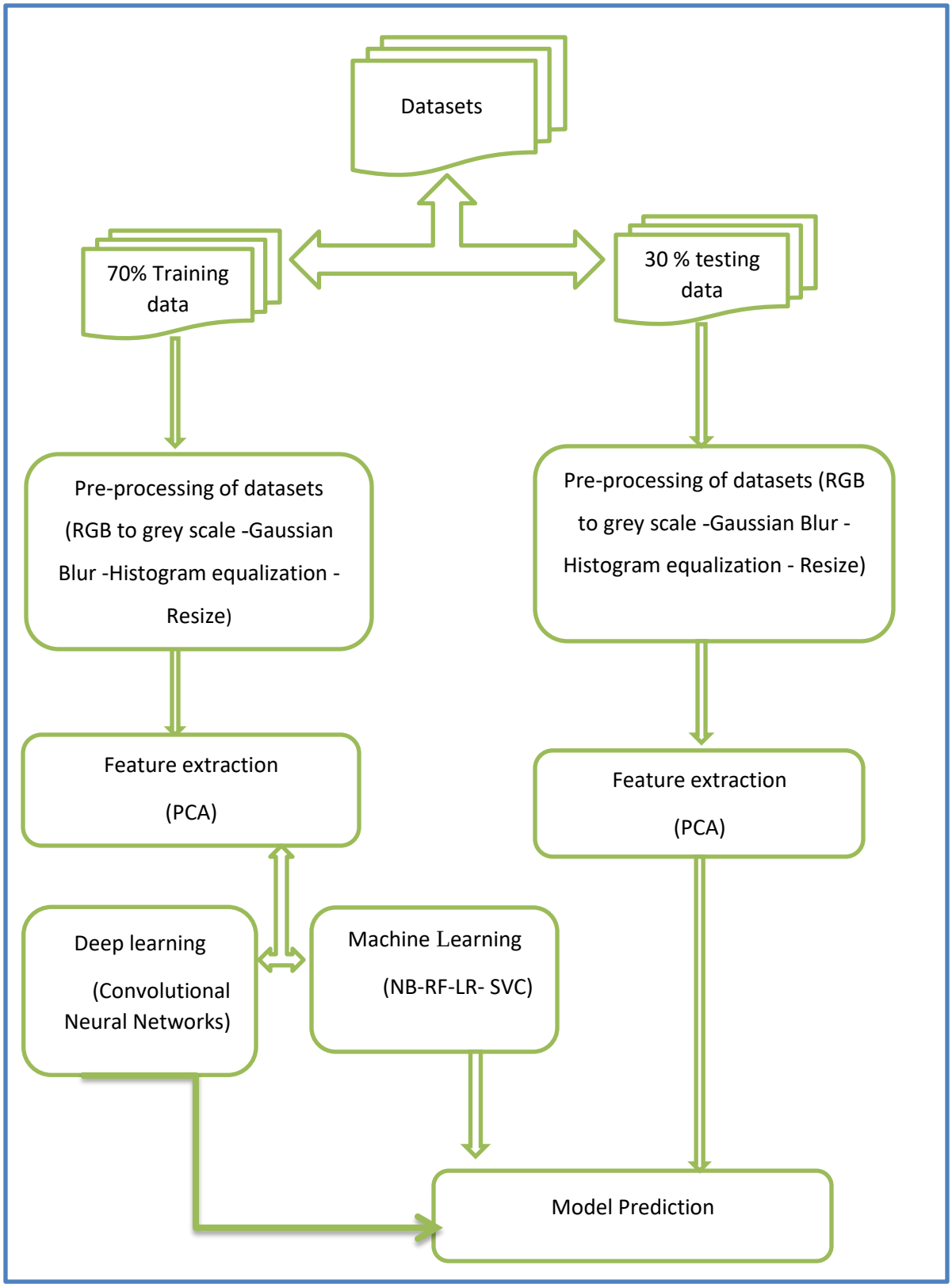

Figure(3.1): Diagram of the Proposed System in Blocks.

3.3 The dataset

ImageNet is a collection of over 15 million high-resolution photos online that have been identified and organized into around 22,000 categories. The images were gathered from the internet and tagged by human laborers using Amazon's Mechanical Turk crowd-sourcing tool, which was made possible by the generosity of Amazon. Because of the widespread use of dermatoscopy [72][73], most skin cancer research focuses on dermoscopy images of skin cancer. For example, the HAM10000 data set [74] is a vast collection of multi-sources dermoscopy images of typical skin images assembled from many sources. Each of the seven forms of skin cancer represented in the data set has 10015 multiple dermoscopy images: basal cell carcinoma, malignant melanoma, non-melanoma melanoma, malignant melanoma, and melanoma. When evaluating the model's performance, it is necessary to use distinct images for the training and test or validation sets.

This dataset contains a balanced dataset of images of benign and malignant skin moles. The data consists of two folders with 1800 pictures (224x244) of the two types of moles. Where we divided this database into two groups, the first 70% of the data is used in training, and the other 30% is used in the testing process.

Figure(3.2) A selection of skin cancer images from the dataset

3.4 Preprocessing

Preprocessing phase needs to be improved and refined to accommodate the necessary modifications of the inputted images. The preprocessing stage on the skin images must be carried out using several multi-step processes and algorithms before skin cancer detection and feature extraction. This guarantees that the inputted images are appropriately edited and ready for further analysis.

3.4.1 Skin Image Conversion to Grayscale

The reason behind this conversion is the reduction in data used to depict the picture. Unlike images in the RGB color space, which need three channels, grayscale images simply have one channel (Red, Green, and Blue) to be saved and represented as digital images. Grayscale conversion of color photos accelerates processing. Grayscale images provide 256 shades of gray, ranging from white to black, and express intensity as an 8-bit integer. In the image preprocessing stage, each pixel in the inputted skin image, which originally had 24 bits, is transformed into grayscale pixels with only 8 bits. This transformation is achieved using a weighted technique described in Equation (2.1) of Chapter Two.

Algorithm (3.1) illustrates the steps of the Grayscale Conversion.

Algorithm (3.1): The Grayscale Conversion
Input: Colored Skin Image. **Output:** Gray Scale skin Image.
Begin **Step 1 :** With every pixel in the colored skin picture: 1.1: Obtain the Red, Green, and Blue values for this pixel. 1.2: Averages Red, Green, and Blue values as Equation (2.1) defines. **Step 2:** Replace the original red, green, and blue values with the gray value producing a Gray skin image. ***END***

3.4.2 Gaussian Blur

Gaussian blur enhances skin image classification by reducing noise and unwanted details by averaging pixel values, smoothing out images, and reducing high-frequency components. Algorithm (3.2) illustrates the Gaussian Blur steps.

Algorithm (3.2): The Gaussian Blur
Input: Gray-scale skin image. **Output:** blurred image of the same size and type as(input image).
Begin **Step 1:** Check if sigmaY is provided. If not, set sigmaY equal to sigmaX. **Step 2**: Create an empty outputImage with the same size and type as the inputImage. **Step 3**: Check if ksize.width and ksize.height are zero. If true, compute the kernel size based on sigmaX and sigmaY. **Step 4**: Create a Gaussian kernel with size ksize and standard deviations sigmaX and sigmaY. **Step 5**: Iterate over each pixel in the inputImage. **Step 6**: Apply the Gaussian blur operation to the current pixel and its neighboring pixels using the Gaussian kernel. **Step 7**: Store the blurred pixel value in the corresponding position of the outputImage. **Step 8**: Repeat steps 5-7 for all pixels in the inputImage. **Step 9**: Return the outputImage, which is the blurred image. ***END***

3.4.3 Histogram Equalization

The gray image's contrast is improved by applying the cumulative histogram equalization technique, known for its effective performance in histogram equalization. This image preprocessing stage follows the steps outlined in Algorithm (3.3).

Algorithm (3.3): Histogram Equalization

Input : Grayscale image
Output : Image with enhanced contrast using histogram equalization

Begin

Step 1: Create an empty histogram matrix of size 256 to store The frequency of each Gray -level intensity.

Step 2: Create an empty cumulative histogram array of size 256.

Step 3: Create an empty mapping array of size 256 to store the mapping of original gray-level intensities to new values.

Step 4: Calculate the histogram of the inputImage by iterating over each pixel: - Increment the frequency count in the histogram array at the corresponding gray-level intensity.

Step 5: Calculate the cumulative histogram by summing the frequencies in the histogram array.

Step 6: Calculate the mapping array by normalizing the cumulative histogram values: - Iterate over each intensity from 0 to 255.

Step 7: Create an empty outputImage with the same size and type as the inputImage.

Step 8: Apply histogram equalization to each pixel in the inputImage: - Get the original intensity value of the pixel. - Look up the corresponding mapping value from the mapping array. - Set the pixel value in the outputImage to the mapped intensity value.

Step 9: Return the outputImage

END

3.4.4 Image Resizing

Image resizing involves altering image dimensions by changing rows and columns. The resized image retains content but has altered dimensions for better presentation, compatibility, and analysis. Algorithm (3.4) gives detailed instructions.

Algorithm (3.4): Resize the Image

Input : Gray-scale Image .
Output: Resized Image

Begin

Step 1: Input the image and the desired dimensions (newWidth and newHeight) for resizing.

Step 2: Calculate the scaling factors for width and height:

- Calculate the width scaling factor by dividing the newWidth by the original image width.
- Calculate the height scaling factor by dividing the newHeight by the original image height.

Step 3: Create a new empty image with the desired dimensions (newWidth and newHeight).

Step 4: Iterate over each pixel in the new image:

- Calculate the corresponding position in the original image by dividing the current pixel coordinates by the scaling factors.
- Use interpolation or other techniques to determine the new image's pixel value based on the original image's calculated position.
- Assign the calculated pixel value to the corresponding pixel in the new image.

Step 5: Repeat step 4 for all pixels in the new image.

Step 6: Return the resized image as the output.

END

3.5 Feature Extraction Phase of skin cancer Images

Feature extraction involves reducing the amount of resources required to describe a large amount of data. Feature extraction from given data is a critical problem for the successful application of machine learning. Generally, skin cancer recognition is a high-dimensional data set classification problem, it needs to perform data dimension reduction task. These features are used to classify the skin cancer. The is global or "holistic" approaches, which takes a holistic view of the recognition problem, and holistic feature extraction of skin cancer images.

PCA is a common statistical method using a holistic approach to find patterns in high dimensional data. The purpose of PCA is derived from the information theory approach, which break down skin cancer images into small sets of characteristic feature images called Eigenskincancer which used to represent both existing and new skin cancer. The statistical information published in the area of skin cancer recognition technology utilizing the PCA method reveals the significance of using this method for identifying and verifying skin cancer features. The purpose of PCA is derived from the information theory approach, which break down facial images into small sets of characteristic feature images called Eigen skin cancer which used to represent both existing and new skin cancer. In PCA method, the 2-Dimensional skin cancer image matrices must be transformed into a 1-Dimensional vector. The 1-Dimensional vector can be either row or column vector. Algorithm (3.5), illustrate the PCA feature extraction for skin cancer image steps.

Algorithm (3.5): **PCA Algorithm**

Input: Resized image
Output : Feature Vectors

Begin

Step 1: read Skin cancer image .

Step 2: Standardize the data\\ This step ensures all features have a similar scale.

- Standardize the dataset by subtracting the mean from each feature and dividing it by the standard deviation .

Step 3: Calculate the covariance matrix.

- demonstrates how to do the covariance matrix calculation. for the uniform data.

Step 4: The eigenvalues and eigenvectors ought to be determined.:

- To determine eigenvectors and eigenvalues of the covariance matrix, perform an eigendecomposition .

Step 5: Choose the essential elements:

- Arrange the eigenvectors in descending order according to the respective eigenvalues .
- Pick the top k eigenvectors that effectively capture the data's greatest variation .
- The primary components are these eigenvectors .

Step 6: Project the data onto the principal components:

- Transform the original data onto the new feature space formed by the selected principal components.
- This is done by taking the dot product between the standardized data and the eigenvectors.

End

3.6 Machine Learning Classification Algorithms

3.6.1 Support Vector Classifier

Potent Machine Learning technique ideally suited for binary classification applications is the Support Vector Classifier (SVC). It operates by locating an ideal hyperplane that maximally divides the data points from several classes.

Training the SVC model on the extracted features can effectively classify new skin cancer images into cancerous or non-cancerous categories.This proposal's

combination of PCA and SVC enables effective feature extraction and classification for skin cancer analysis. PCA helps reduce the dataset's dimensionality, while SVC leverages the extracted features to classify skin cancer images accurately. By leveraging the strengths of these techniques, the proposal aims to improve the accuracy and efficiency of skin cancer detection, ultimately contributing to early diagnosis and improved treatment outcomes. Algorithm (3.6) illustrates the demonstration of applying the classifier SVC to the features of PCA.

Algorithm (3.6): SVC Algorithm

Input: Feature Vectors
Output: Classification

Begin

Step 1: Read Skin cancer images.

Step 2: # Creating training and test split

- K_ train, K_ test, j_ train, j_ test = train_ test_ split(K, j, test_ size=0.3, randomly_ state = 1, stratify = j)

Step 3: # Feature Scaling

- ss = Standard Scaler ()
- ss. fit(K_ train)
- K_ train_ std = ss. transform(K_ train)
- K_ test_ std = ss. transform(K_ test)

Step 4: # Training an SVM classifier using the SVC class

- SVM = SVC(kernel= 'linear' , randomly_ state=1, C=0.1)
- SVM. fit (K_ train_ std, j_ train)

Step 5: # Mode performance

- j_ pred = svm. predict(K_ test_ std)
- print ('Accuracy: %.3f' % accuracyy_ score(j_ test, j_ pred))

END

3.6.2 NB algorithm

The NB algorithm has been a simple probabilistic classifier that calculates a set of probabilities by counting the frequency and combinations of values in a given data set. It used Bayes Theorem to predict the probability that a given feature set belongs to a particular label as shown in algorithm

Algorithm (3.7): NB Algorithm

Input: Feature Vectors
Output: classified with NB classifier

Begin

For each class in dataset do # compute

p(c) $\mathbf{P(c) = Nc/ N}$

$\boldsymbol{Nc}$ Represent the total count of particular class ing dataset

$\boldsymbol{N}$ Represent the total count of classed in dataset.

For each word in class #compute p(w/c)

Where P (d/c):- con. Pro / likelihood where w is word attribute and c is class.

+1 represents the Laplace smoothing

Count (w,c) represents the total count of the word attributes that occur in a class.

Count(c) represents the total count of the word attributes, in specific class occurring in a training dataset.

$\mathbf{p(w|c) = count(w,c)+1 / count(c)+|v|}$

|v| represents the vocabulary, the total count of various word attributes in the training

For each class compute bays theorem #P(C/W)

Calculate P(POS/W)=P(pos)*P(W1/class pos)* P(W2/class pos)…

*P(Wn/class pos)

Calculate P(NEG/W)=P(neg)*P(W1/class neg)* P(W2/class neg)…

*P(Wn/class neg)

Assign document to class which is of a higher possibility

End for

End for

End for

END

3.6.3 Random Forests (RF)

Algorithm (3.8): RF Algorithm

Input: Feature Vectors
Output: Classification

Begin

1: Load train data from the directory to model

2: Load test data from the directory to model

3: Input image shape (300,300,1), batch size = 32 Feature Map Process (Feature Extraction stage)

4: Add Conv2D with random kernel = 4, kernel size = (5*5)

5: Add batch normalization layer

6: Add ReLU; (It neglects negative values and maintains only positive ones)

7: Add Conv2D with random kernel = 8, kernel size = (5*5)

8: Add batch normalization layer

9: Add ReLU

10: Apply MaxPool2D with size = 2,2; st = 2

11: Add Conv2D with random kernel = 10, kernel size = (5*5)

12: Add batch normalization layer

13: Add ReLU

14: Add Conv2D with random kernel = 16, kernel size = (3*3)

15: Add batch normalization layer

16: Add ReLU

17: Apply MaxPool2D with size = 2,2; st = 2

18: Add Conv2D with random kernel = 32, kernel size = (3*3)

19: Add batch normalization layer

20: Add ReLU 21: Apply MaxPool2D with size = 2,2; st = 2

22: Add Conv2D with random kernel = 64, kernel size = (3*3)

23: Add batch normalization layer

24: Add ReLU

25: Apply MaxPool2D with size = 2,2; st = 2 Classification stage

26: Add RF classifier

27: Computing loss between the output and the true class Iterations

28: Repeat steps from 1 to 27

29: Apply Adam with a learning rate (0.001) to update weights at steps and update kernel at steps

30: For each 32-batch size Do

31: Test model on the test dataset and compute test loss; test accuracy

32: Save model weight in file directory depending on test accuracy improvement

33: batch size ++, epochs ++

34: Until epochs = 25

END

3.6.4 Logistic Regression algorithm (LR)

LR has been used to determine the output or result when there were one or more than one independent variables. The output value might be in form of 0 or 1 i.e. in binary form as shown in algorithm.

Algorithm (3.9): Logistic Regression Algorithm

Input: Feature Vectors.
Output: classified with LR classifier.

Begin

Foe each training instance:

1)Calculate a prediction using the current values of the coefficients

$$\boldsymbol{prediction} = \mathbf{1} / (\mathbf{1} + \boldsymbol{e}\text{^}(-(\boldsymbol{b0} + \boldsymbol{b1} * \boldsymbol{x1} + \boldsymbol{b2} * \boldsymbol{x2})))$$

2)Calculate new coefficient values based on the error in the prediction

$$\boldsymbol{b} = \boldsymbol{b} + \boldsymbol{alpha} * (\boldsymbol{y} - \boldsymbol{prediction}) * \boldsymbol{prediction} * (\mathbf{1} - \boldsymbol{prediction}) * \boldsymbol{x}$$

Where b is the coefficient it has been updating

Prediction is the output of making a prediction using the model.

Alpha is parameter that you must specify at the beginning of the training run (might be in the range 0.1 to 0.3).

End for End

END

3.7 Deep Learning Proposal

The 27 layers that make up the proposed CNN model will be defined in Figure (3.2), which will give a detailed introduction to it :

- **Eight** convolutional layers for type 1D feature extraction.
- **Eight** LeakyReLU 1D layers .
- **Seven** 1D layers with Maxpooling .
- **Three** The (Dense) layer represents a fully connected layer **.**
- **One** flat layer**.**

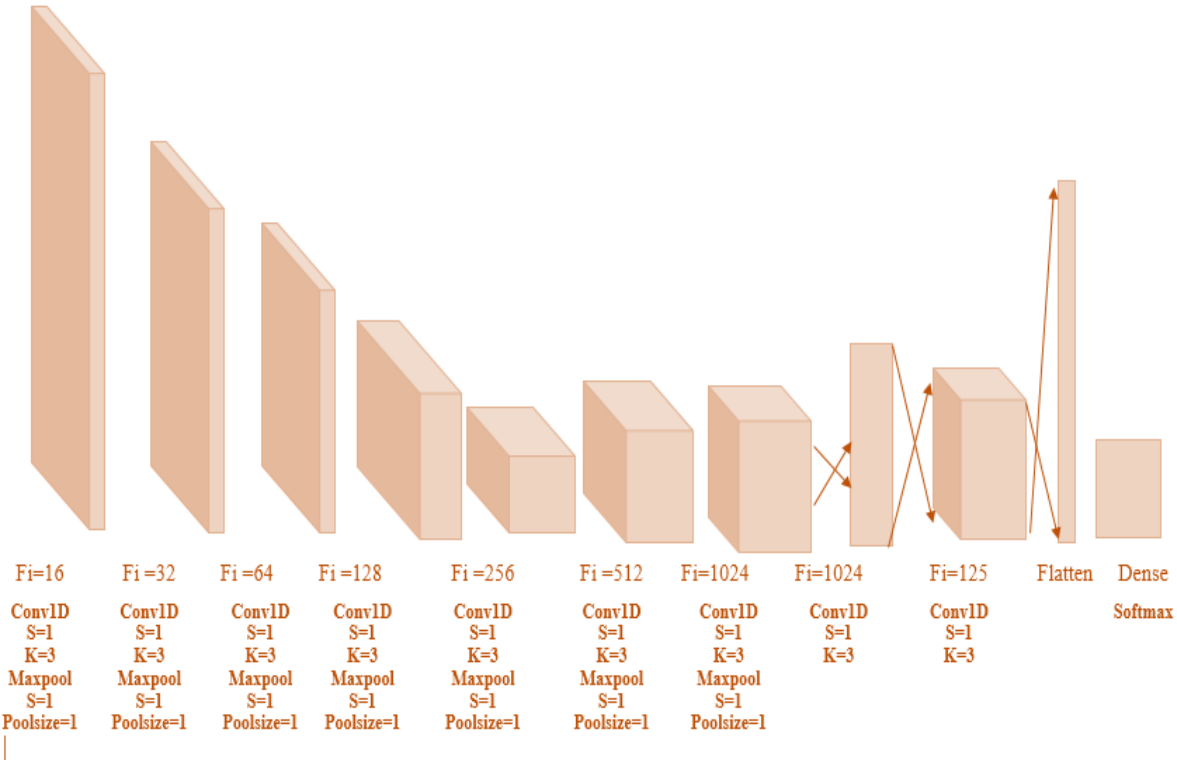

Figure (3.3): The Proposed CNN Model.

Algorithm (3.10) provides a more detailed explanation of the layers that are incorporated into the proposed deep learning algorithm. This simple representation of our algorithm was developed to yield high accuracy and superior results.

Algorithm (3.10): Deep Learning Algorithm

Input: Feature Vectors
Output: Classification

Begin

Step 1: load data train from the directory of model
Step 20:load data test from the directory of model
Step 3: add Conv1D filters=16 , kernel size=3, input shape=(400,1)
Step 4: add LeakyReLU alpha=0.3
Step 5: add MaxPooling1D pool size = 1, strides=1
Step 6: add Conv1D filters = 32 , kerne1 size = 3, strides = 1
Step 7: add LeakyReLU alpha=0.3
Step 8: add MaxPooling1D pool size = 1, strides=1
Step 9: add Conv1D filters = 32 , kerne1 size = 3, strides = 1
Step 10: add LeakyReLU alpha=0.3
Step 11: add MaxPooling1D pool size = 1, strides=1
Step 12: add Conv1D filters = 128 , kerne1 size = 3, strides = 1
Step 13: add LeakyReLU alpha=0.3
Step 14: add LeakyReLU alpha=0.3
Step 15: add MaxPooling1D pool size=1, strides=1
Step 16: add Dense (128, activation = "linear")
Step 17: add Conv1D filter = 256 , kernel size=3 , strides=1
Step 18: add LeakyReLU alpha=0.3
Step 19: add MaxPooling1D pool size=1, strides=1
Step 20: add Conv1D filter = 512 , kernel size = 3 , strides =1
Step 21: add LeakyReLU alpha=0.3
Step 22: add MaxPooling1D pool size=1, strides=1
Step 23: add Conv1D filter = 1024 , kernel size = 3 ,strider = 1
Step 24: add LeakyReLU alpha=0.3
Step 25: add MaxPooling1D pool size=1, strides=1
Step 26: add Dense (1024 activation = "linear")
Step 27: add Conv1D filter = 50 , kernel size =3 , strides = 1 , activation='linear'
Step 28 : add Flatten()
Step 29: add Dense (2, activation = "softmax").

END

Learning rate = 0.0001.
Epochs = 100: number of iterations.
Batch size = 64: a batch of the image sample

Chapter Four

Results and Discussion

Chapter Four

Results and Discussion

4.1 Introduction

The experimental findings from the suggested system of skin cancer images are covered in this chapter. The methods and practices for implementing skin cancer image results were previously discussed in chapter three. First, the environment where the system is implemented is described, together with all the platforms and programming languages that are employed. The suggested system's success will then be demonstrated through the presentation and discussion of the findings from each phase.

metrics can be used to describe how well a neural network classifier performs in the detection of melanoma skin cancer. Sensitivity and specificity are crucial criteria for medical image diagnosis. They will affect this thesis' performance assessments in addition to accuracy.

The experimental findings and the most popular methods for diagnosing melanoma of the skin are introduced in this chapter.

4.2 Environment Description

The implementation environment description is significant in evaluating the proposed system's behavior and performance and how it works. The charts for the proposed system's implementation will be shown in this section. The programming languages used to accomplish the proposed system function are Python programming language and visual studio programming language, the hardware specifications were satisfied by the Intel (R) Core(TM) i7 CPU, 320GB Hard Drive, and 8GB of random access memory (RAM).

4.3 Implementation Results

The proposed detection system of melanoma skin cancer has been tested on 3300 images to diagnose melanoma, whether benign or malignant. A set will be discussed and implemented, and each stage of the system will be fully explained taking users through preprocessing, using PCD algorithms for feature extraction, transforming input data into informative representations, and a deep CNN for classification. An illustration of a skin image, Figure (4.1) displays the data that has been entered into the proposed system.

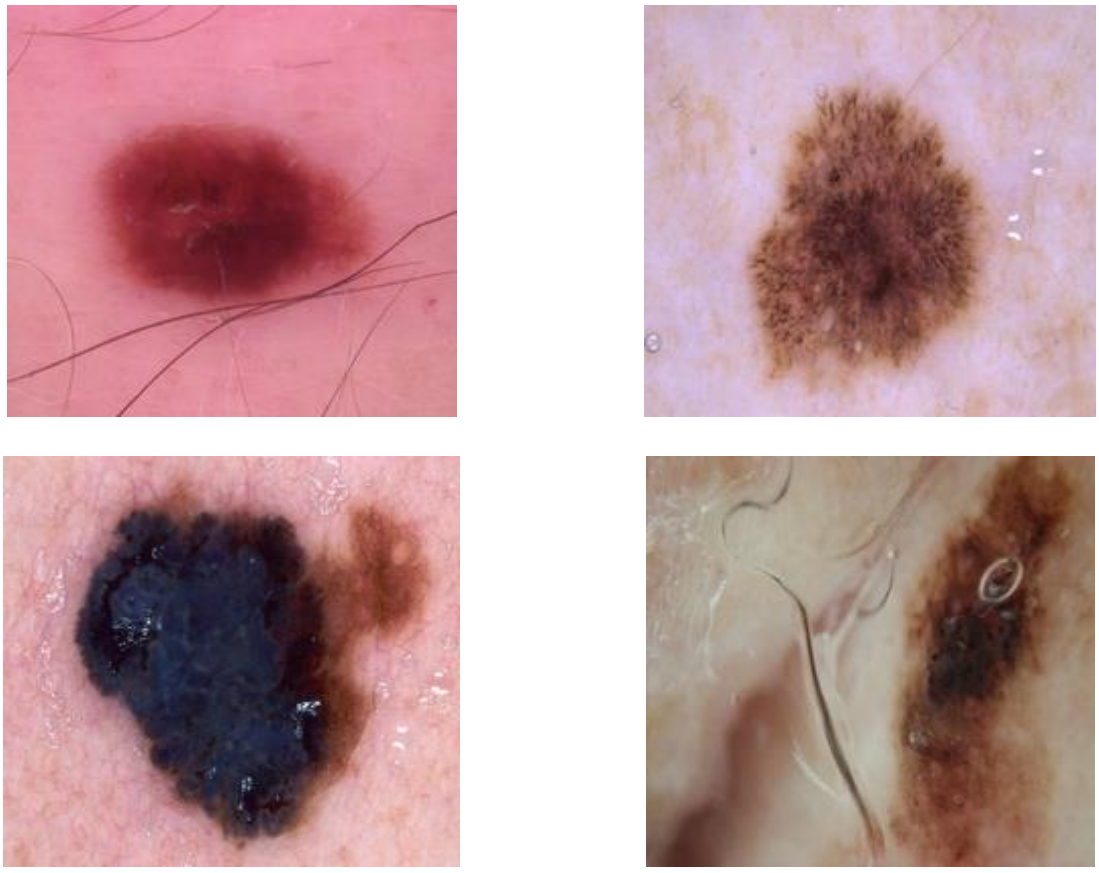

Figure (4 . 1): Examples of Skin

4. 4 Results of the Preprocessing Phase

The preprocessing of the skin images is the first phase in the proposed system. The classification phase consists of the following four processes, which are part of the preprocessing, to provide accurate skin images to work with:

4.4.1 Greyscale Converting

the first step in the preprocessing is to convert the image from the colored image into greyscale image. The conversion process will make the image takes less storage and less channels in representation and this is very important in the classification procedure due.

The proposed system uses grey scale color space for skin images, as shown in Figure (4.2).

Figure (4.2): Converted Skin Images to Greyscale.

4.4.2. Gaussian Blur

This method of blurring creates a smooth blur that simulates the appearance of a translucent screen when applied to an image. Figure (4.3) illustrates a skin image sample after the effective Gaussian Blur.

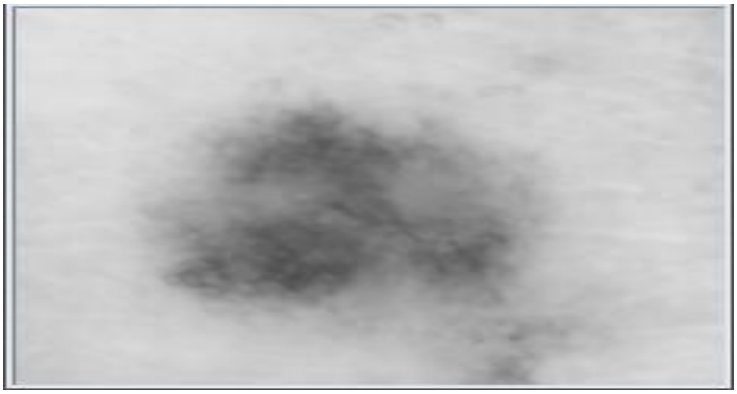

Figure (4.3): Gaussian Blur of Skin Images

4.4.3. Histogram Equalization

The histogram equalization is applied to the skin images after converting them to grey color and Gaussian blur to improve their differences to Clarify the image's details, It will aid in the phase of detection. Figure (4.4) shows an example of results from skin images after applying histogram equalization.

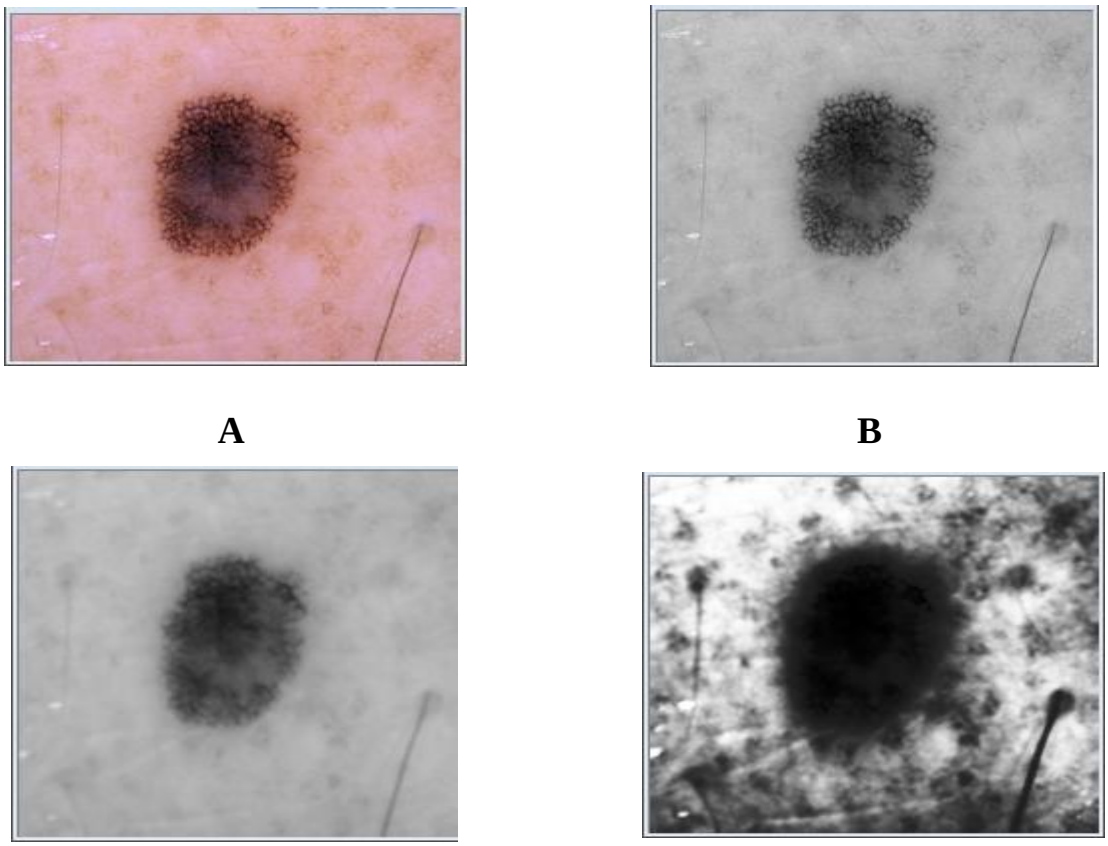

Figures (4.4): provide an example of a benign melanoma image after preprocessing. A) The original image. B) Convert to grayscale. C) using a Gaussian blur. D) Applying Equalization of the histogram.

4.4.4. Resize Skin Cancer Image

The next step the resizing process in which the digital skin grey image will attain anew dimensional value in which it smaller. All images were reshaped with 20*20 distances. Figure (4.5) illustrate the skin image after resizing process.

A **B**

Figure (4.5): Resulted in Skin Images after Resizing. (A) Original Images (B) Resized Images.

4.5. Feature Extraction Phase

Feature extraction is the next phase in this thesis. The approaches and algorithm are applied to perform the extraction of features, which is PCA. The results obtained from applying the feature extraction algorithm will be described and shown in the next figures and tables mentioned in Figure (4.6).

a381	a382	a383	a384	a385	a386	a387	a388	a389	a390	a391	a392	a393	a394	a395	a396	a397	a398	a399	a400
14.76253	-17.3344	10.27419	2.028348	-27.675	-6.30847	-7.92737	5.802978	-0.92038	-23.6965	-9.562	-0.2926	9.087906	26.68911	-15.6343	0.804055	1.566377	2.314076	4.066698	11.49948
-11.6879	24.03366	2.937776	5.927745	4.222504	3.16089	-10.951	-1.81463	3.438719	-0.35597	-3.07438	-4.72006	-7.78498	4.87938	-10.9749	-5.2135	8.465978	4.549467	-9.4062	-1.08059
34.47681	-5.20655	-13.2416	3.281537	7.892304	9.207171	-3.42111	1.453076	1.794092	-1.0273	-2.54451	15.18866	-17.8561	3.630944	16.31557	-28.3333	-1.6798	-3.08344	-2.625	-0.70726
4.418706	4.031917	5.228168	-17.1786	12.05963	-2.8222	12.45336	-4.00702	25.71883	0.23706	18.72641	-8.38177	2.952384	21.76719	33.99081	3.207111	3.49911	17.93623	-15.2114	-1.62703
-27.2074	-1.91318	-6.55091	-1.35617	8.357669	-12.4172	7.339037	34.16339	-8.65755	23.14567	0.706346	-11.0875	-1.49745	10.68097	-30.1432	-17.0786	5.529777	-13.0906	-3.18693	-16.1945
-6.33035	-28.3048	-34.4691	8.372972	15.66363	-14.3633	-13.064	3.560074	-14.6224	-57.4931	13.63167	-9.33486	13.80798	-7.41826	4.525979	24.79968	-3.36849	-8.80117	8.427239	-14.7858
-15.4709	5.402616	3.932871	19.52397	-0.42923	8.779011	-1.63719	20.78956	-1.10165	6.125384	-13.8487	-8.62936	-0.99979	5.544383	9.049147	8.926648	37.33707	15.70435	3.790855	27.16568
18.52991	-0.31351	-0.96356	-3.14284	9.882903	-5.75112	-4.46004	14.71643	10.25899	-18.431	-9.64655	-4.14359	1.85317	-4.34002	-18.1983	-6.0189	-9.23777	3.130947	-8.41741	-5.58497
13.8421	-6.95896	0.217266	-7.86133	4.798677	-8.67194	-0.68331	-6.71212	-14.7787	-8.8353	-6.58186	-0.00585	3.211255	20.03826	-21.3461	23.20198	-0.04612	18.94709	-4.01623	10.95939
-3.51477	-47.7782	-13.4309	-5.4576	30.49836	42.86537	15.02325	-7.71498	-7.43863	-7.76339	-27.4838	30.25879	14.8458	-18.6916	15.09611	-6.33468	17.42593	-12.6268	-21.1963	14.99776
26.43313	-5.39659	-4.63628	15.87696	-8.49464	5.830369	9.662178	13.717	2.746137	-4.60964	19.41437	19.31713	4.868535	-0.82415	14.55513	24.87839	-0.41104	6.479674	1.039426	-11.614
-45.5857	19.41328	2.765816	-26.5034	-21.7381	2.676895	-5.91002	7.466089	11.06155	-34.7634	-1.66934	-4.33203	3.192162	25.6134	1.62938	7.538471	6.992625	-5.79094	4.791255	3.577271
-2.00845	-4.56903	-12.4964	2.542468	22.03709	33.85185	3.905253	-6.0108	-12.6455	-2.09238	1.249668	-11.9613	-27.1409	14.76615	7.601946	10.04027	11.80472	-6.834	-5.58879	-4.06882
9.133621	13.8284	0.375431	-24.3159	-17.1483	19.19519	-5.46894	-11.8548	-20.79	-2.74558	-2.61564	6.486503	-4.41776	-8.98439	4.136956	2.805325	6.904111	-6.79924	21.64303	-7.99706
-29.6467	-0.2251	5.465292	8.721544	2.422486	-7.13854	-4.46405	1.39755	-5.04257	7.609091	-0.32303	-0.76177	-6.31662	-0.45962	-7.68836	6.385246	-20.8274	4.262892	9.70969	12.21537
24.46154	10.65641	-1.54009	0.312562	12.71462	1.576992	-21.686	4.26282	3.0421	-11.415	-1.44592	-15.4685	12.38427	18.93236	-10.8833	7.699759	12.38637	8.117228	-11.3513	10.30014
4.73221	10.83835	-10.8786	-17.405	4.579663	25.39272	-22.275	-15.8061	20.49096	-3.08474	-0.96159	7.57754	2.88779	-2.49575	-9.69517	-23.3551	-18.5654	-9.9318	9.533358	-8.39361
-6.77879	7.462543	0.122428	2.716381	11.44117	-20.909	2.101941	11.83007	-0.96492	-7.21557	3.829538	-10.0595	-11.4687	10.82174	-5.56227	-4.7669	-12.6474	-4.41493	0.866612	-13.42
4.397203	-27.8197	-0.55108	3.384091	2.4842	9.140838	-4.2124	-19.3176	5.519516	20.4085	-29.7342	-5.27551	-5.48507	-5.56074	-1.53225	8.686289	2.143685	7.615272	-1.87999	9.6005
9.362675	30.27145	-42.2866	8.801257	9.494006	13.85627	14.51975	10.60905	-2.72933	-1.83901	-6.87767	-6.94964	16.21489	4.390503	-29.452	-30.8335	-19.9915	4.119437	-9.01427	-1.99691
5.230316	-4.55835	-8.4609	-5.90168	-5.25374	-6.92079	20.88784	3.060967	20.83738	-13.4772	-7.32009	3.474328	2.990368	0.610497	-2.14129	4.53007	0.750948	4.004458	-10.6817	-5.04727
-5.53277	-6.30224	-7.91666	-10.4383	36.62131	-6.68116	-9.87863	-17.2443	8.092858	-13.4024	27.9011	-6.03288	18.16733	11.12173	-9.74866	2.892993	6.474036	-21.6196	-19.6221	-4.35507
-40.2733	1.392588	-10.9696	-22.0645	-27.1664	-28.4488	0.88877	24.65857	0.190888	6.122079	7.788209	-13.1717	-0.26699	3.795714	6.306921	-6.95882	-3.35528	1.595457	14.63452	13.24692
-29.2378	-5.20809	-11.5805	-12.6711	11.21097	-37.9773	-11.1878	12.68966	-15.8915	4.838313	19.1258	-11.2648	2.147455	-17.7262	-21.5748	17.56165	-6.15064	-14.1143	-5.99238	14.87674

-593.021	224.3418	337.7192	22.9628	-113.284	70.31193	-99.7972	-219.934	38.57091	131.4145	84.99365	-10.1628	-103.192	-62.5646	55.29737	105.3665	102.5202	-81.6655	28.85057	-37.1608
-378.325	137.0779	-154.515	91.34506	-568.804	534.5167	-116.785	236.4179	22.16772	-159.127	-102.941	186.3903	-10.6544	-59.0823	-26.8689	-14.7318	75.90187	-174.252	45.49481	80.88014
-296.188	-226.717	124.6765	-175.733	-193.402	-176.267	69.09519	100.6862	24.31471	-72.072	-47.2411	-148.045	15.30807	-265.417	-162.373	64.96188	-35.8835	-23.6571	-67.6588	-9.97879
-564.728	64.52208	-638.483	-224.634	-48.4076	296.219	66.91254	39.85499	63.11744	-81.6816	-40.568	69.18831	-68.5787	-53.5417	43.69467	-61.1915	-9.77999	-112.072	-117.807	-87.1198
-702.841	344.3869	-287.077	-146.713	-61.6984	296.9555	-161.792	-297.215	-80.0185	-56.7946	-156.499	-54.0996	72.02441	-54.1059	-15.7585	25.55675	2.726109	-104.415	-62.552	61.97617
-255.054	-670.927	469.1999	-499.659	-255.686	-212.4	-299.034	-60.2544	-126.635	-57.2061	-6.98069	33.05112	-152.536	87.64482	69.3079	-141.735	-212.025	-272.766	-204.282	-46.2726
-630.701	-559.35	-442.093	-288.938	77.9813	-182.574	230.4635	-89.2462	-4.58269	131.2306	-194.446	-34.7701	12.72574	7.291763	-104.928	-74.9224	-214.056	-17.2863	200.1353	48.32683
-241.354	-386.28	-571.996	307.9587	-498.487	150.4703	131.91	55.28012	111.8693	-289.693	27.6067	-53.0368	-120.715	-260.943	0.661172	-80.0496	26.29827	-116.075	-82.4713	-217.161
1012.361	-26.2778	14.23897	-301.069	-40.4926	-245.698	-292.54	41.79799	-224.739	-19.2359	-95.0358	-157.144	-55.0953	4.395097	-120.633	146.7416	-66.8127	222.8184	-11.5969	63.09141
73.01012	-27.5482	8.552778	-577.557	-65.3627	-217.449	154.6116	-97.5899	60.40869	164.3338	105.3644	-51.9819	148.8085	82.06608	34.17889	-3.87713	-52.6459	64.54277	-196.314	50.39247
-369.647	-158.377	-372.55	0.600747	-171.439	187.4267	150.6842	655.5557	190.8197	-81.3217	-40.9059	195.5511	-46.6356	1.345645	204.3836	140.6584	117.843	-76.0998	-100.552	22.20982
198.1659	46.43913	-145.59	168.2419	223.9185	-215.476	-165.693	417.8381	388.922	-19.9947	22.34356	-62.7864	48.5562	-121.175	16.70703	-104.041	-30.487	89.48083	116.7822	-52.6705
-437.328	14.9603	-272.766	114.1178	137.8501	341.6798	-316.407	-131.656	-343.388	-213.331	105.5694	50.95572	-214.548	94.95524	-148.728	-52.1661	-56.1848	33.37832	-124.609	154.8921
124.0353	-43.5682	-49.7895	-258.483	-55.2984	-37.414	273.1136	221.7236	266.8322	227.3247	61.58682	135.1608	-42.0954	126.6091	-91.578	241.6991	-5.4942	49.98718	-63.6666	0.522158
-116.741	21.77442	-274.356	-12.2604	74.72173	-120.868	211.0508	-353.321	-39.7902	-36.0799	27.10558	-92.7013	18.99033	203.6051	77.1073	26.27678	-7.41534	13.43347	28.5562	-197.582
-223.682	510.2916	20.38082	-609.838	-3.29258	-357.82	-296.502	-15.7103	-67.0145	76.4384	27.69568	-99.1863	-135.681	-9.22235	133.0114	-24.986	56.31406	76.02696	63.40964	167.4011
390.8614	-268.925	355.0581	-484.43	-487.09	-209.355	-48.0424	56.08605	96.74996	-25.942	-76.548	-27.401	-290.798	-20.0513	125.4083	10.1766	-190.33	-9.15593	185.3478	-101.793
-324.779	-635.396	392.3864	-242.036	-187.226	-113.311	11.69911	4.088949	30.27312	67.36558	38.84657	280.4092	34.32686	220.5602	132.9472	145.5559	312.6069	93.7695	14.25238	-368.475
15.24167	-3.88945	130.0236	-130.311	589.4917	-88.4809	216.9699	139.9147	-270.602	-246.109	-260.103	367.2356	-144.562	187.1954	-62.9804	148.7622	-127.523	-176.982	-182.068	26.18092
-184.118	-346.946	209.1577	138.0397	-339.984	194.9383	184.8181	-17.7228	4.313854	-57.5662	137.9479	-207.815	60.82733	90.2014	36.97339	70.41446	-93.4347	11.72736	-1.45317	-107.474
-712.195	192.2574	-223.124	-201.717	-66.0233	481.2614	-95.8344	-40.6923	-100.018	271.4737	143.2057	202.0928	-9.34474	120.1372	170.2763	-109.959	-131.54	-25.9213	109.3468	-46.6437
-364.288	236.7903	238.1444	-190.672	273.9097	58.16633	179.9983	225.6647	-179.576	178.9175	167.3438	-197.098	410.118	-159.647	14.57778	199.4221	74.0636	38.07024	-77.0951	-330.782
353.6086	86.40113	405.4878	36.85788	-89.0004	66.28485	-0.86155	-108.358	-71.9469	-31.2992	-48.4301	72.82181	103.2827	21.91739	83.32788	60.32624	27.85058	-98.5418	-40.2503	71.48763
345.526	-221.503	-138.264	273.7257	132.9972	143.673	110.4419	35.80515	-113.91	8.811579	74.68284	105.5652	-65.4065	55.56822	180.6719	-55.5451	-160.216	48.2751	87.74762	32.56394
-73.9057	-261.226	-300.486	572.291	-549.769	24.44828	90.02284	89.32863	-92.7575	-103.188	224.8451	-28.7697	34.21869	-19.5334	-186.801	-99.8515	31.55004	118.3454	63.40085	-103.744

Figure (4.6): Samples of Resulted Features Extracted using PCA

4.6 Classification Phase using (NB ,LR,RF and SVC)

The classification is a significant point of the presented system in this thesis, five machine learning algorithms were utilized for training the features and testing them to compare the obtained results to the results attained using the CNN deep learning algorithm. In this part of thesis, a description is obtained about the results of applying both of NB,LR,RF and SVC machine learning algorithms for classify the features obtained from the previous described feature extraction algorithms which include PCA. Table (4.1-4), will describe the result of implemented NB,LR,SVC and RF, with PCA respectively.

Table (4.1): The experimental results of implemented NB algorithm

Classes	Precision	Recall	F1-score	Accuracy
0 (Benign)	0.68	0.66	0.67	
1 (Malignant)	0.54	0.56	0.55	
All class				0.62

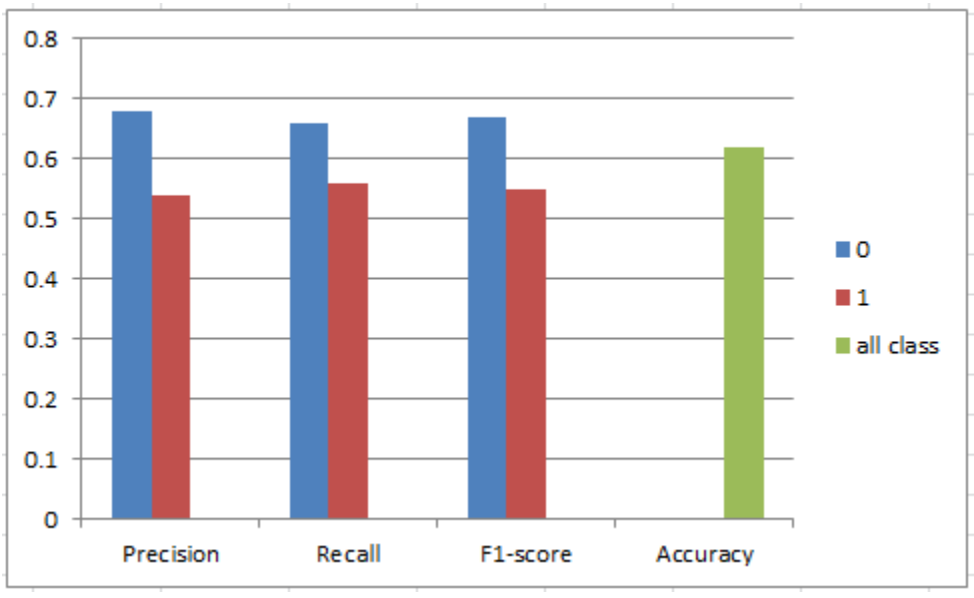

Figure (4.7). Results of implemented NB algorithm

Table (4.2): The experimental results of implemented LR algorithm

Classes	Precision	Recall	F1-score	Accuracy
0 (Benign)	0.75	0.73	0.74	
1 (Malignant)	0.63	0.66	0.64	
All class				0.70

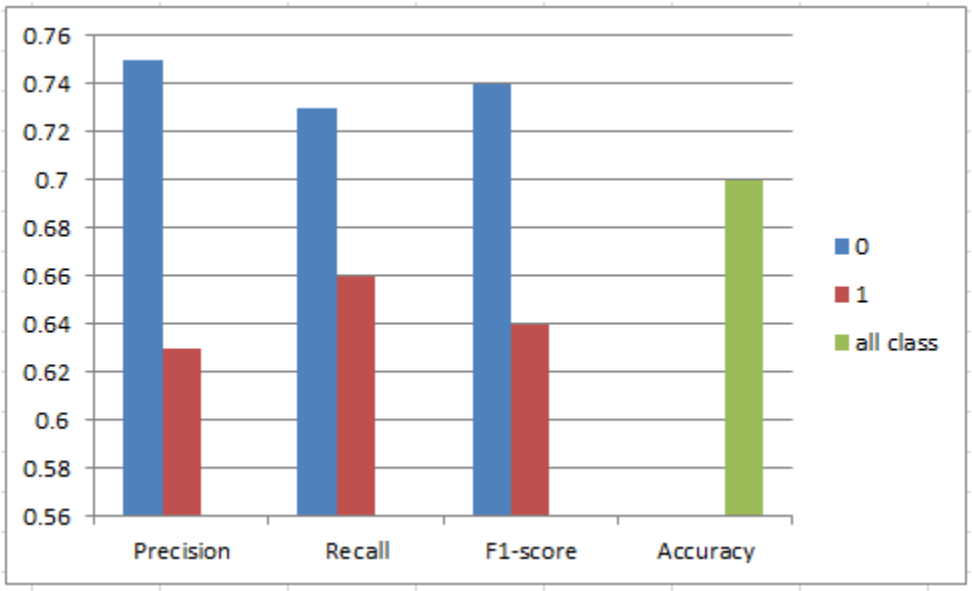

Figure (4.8). Results of implemented **LR** algorithm

Table (4.3): The experimental results of implemented RF algorithm

Classes	Precision	Recall	F1-score	Accuracy
0 (Benign)	**0.75**	**0.73**	**0.74**	
1 (Malignant)	**0.64**	**0.66**	**0.65**	
All class				**0.70**

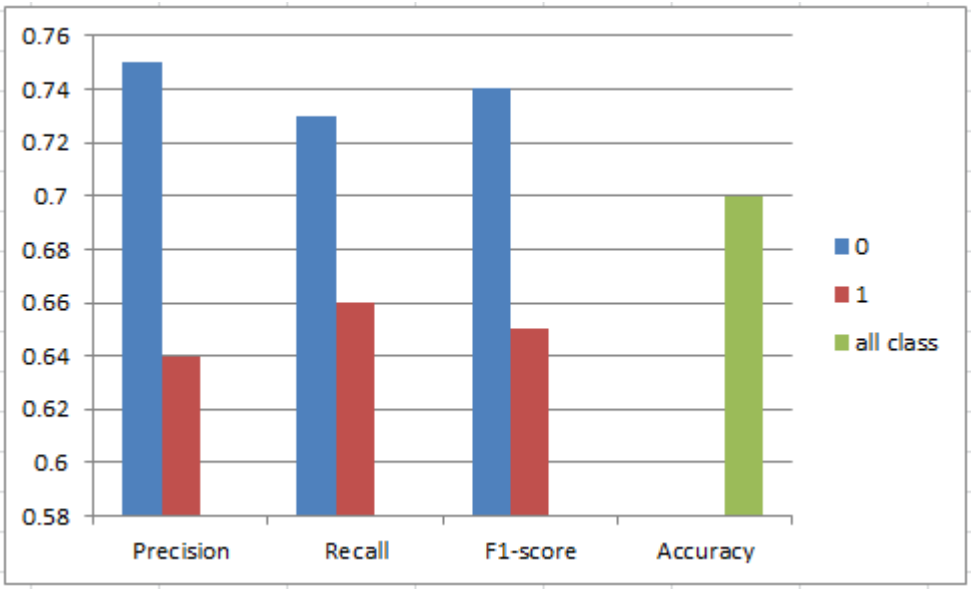

Figure (4.9). Results of implemented **RF** algorithm

Table (4.4): The Experimental Results of Implemented SVC Algorithm

Classes	Precision	Recall	F1-score	Accuracy
0 (Benign)	0.75	0.76	0.75	
1 (Malignant)	0.69	0.68	0.68	
All class				0.72

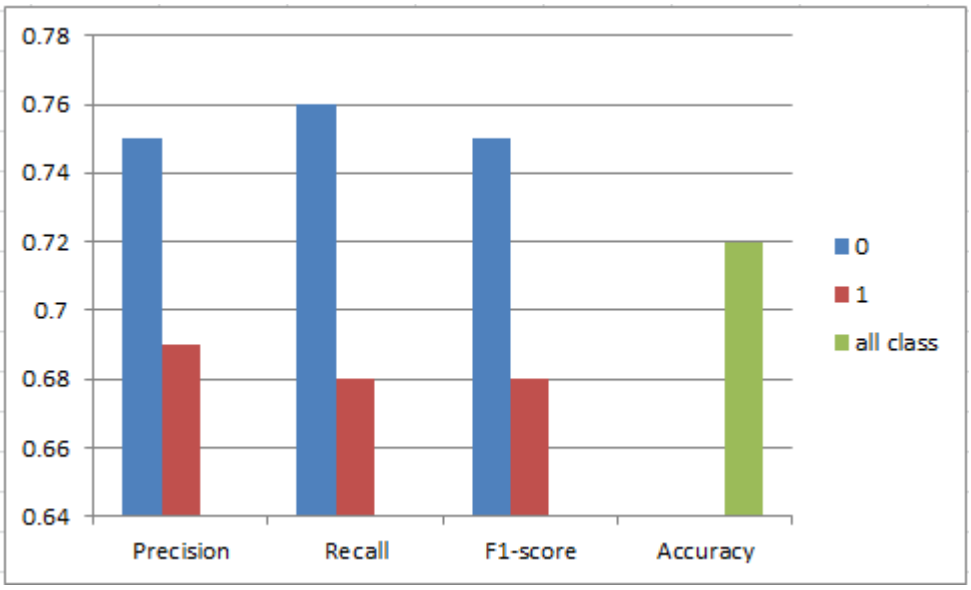

Figure (4.10): Results of Implemented SVC Algorithm

4.7 Classification using CNN

To compare the resulting findings to those produced using the CNN deep learning method, machine learning algorithms were used to train the features and test them. The results of applying both MobileNet and Deep learning methods for categorizing the characteristics derived from the previously stated feature extraction algorithms, including PCA, are given in this section of the thesis. Table (4.2), and Figure (4.8) show MobileNet-CNN implementation outcomes.

Table(4.5): The Experimental Results of Applicated Proposed Deep Learning,

Classes	Precision	Recall	F1-score	Accuracy
0 (Benign)	99.9	99.9	99.9	
1 (Malignant)	99.9	99.9	99.9	
All class				99.9%

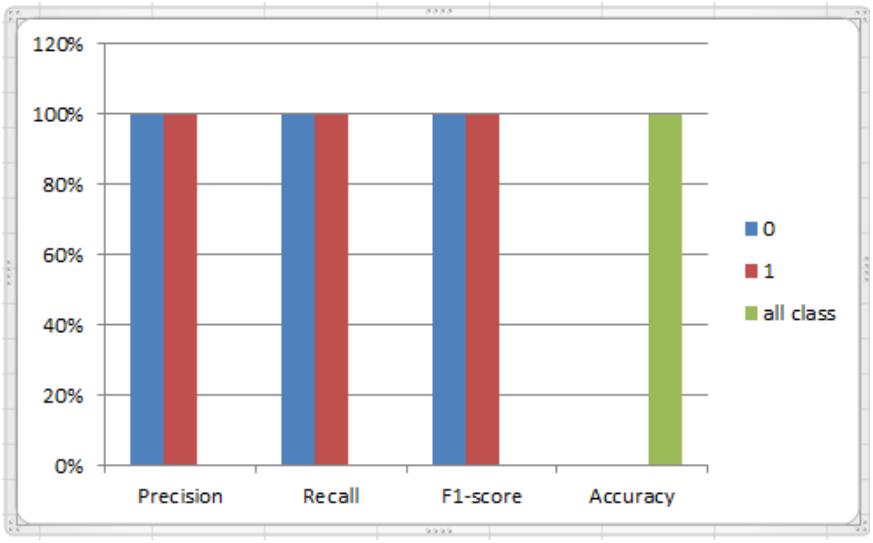

Figure (4.11): Results of Implemented Proposed Deep Learning

4.8 Discussion

This thesis aimed to develop a system to identify skin cancer early, specifically targeting malignant melanoma, to enable early diagnosis and assist doctors in providing timely and accurate diagnoses. The goal was to improve the reliability of diagnostic results while saving time for patients and medical professionals. Timely and accurate diagnoses can lead to more effective interventions and preventive measures, ultimately reducing skin cancer cases.

We first trained more than one of the machine learning algorithms, which gave unsatisfactory results, as the accuracy does not exceed 72%.

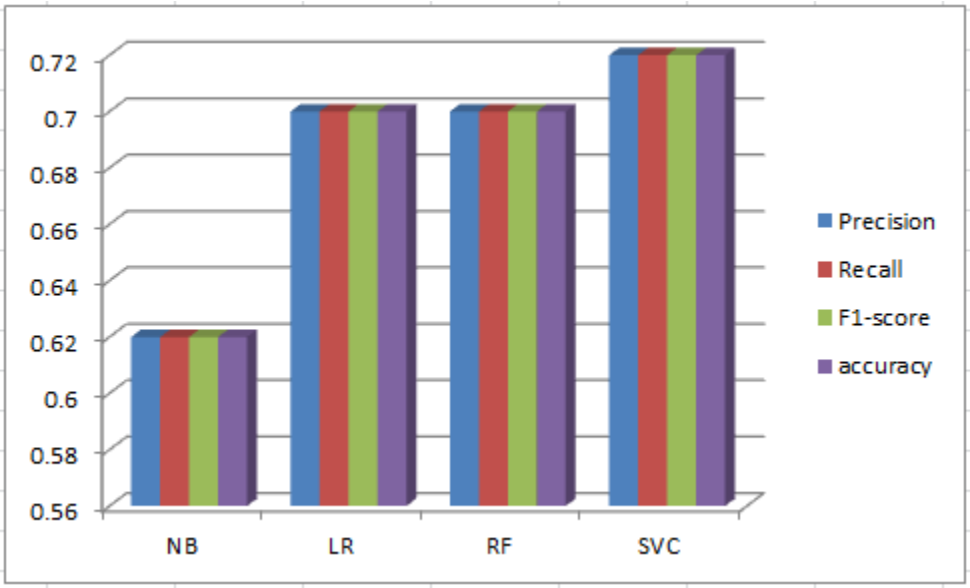

Figure (4.12). Results of implemented **Machine Learning** algorithm

So, a deep learning system has been proposed. This system gave us a perfect accuracy of 99.9%.

This accuracy has not been reached in previous work classifying melanoma skin cancer.Figure (4.13) displays a chart showing the comparison between the algorithms trained in the system, depending on the accuracy obtained from each algorithm.

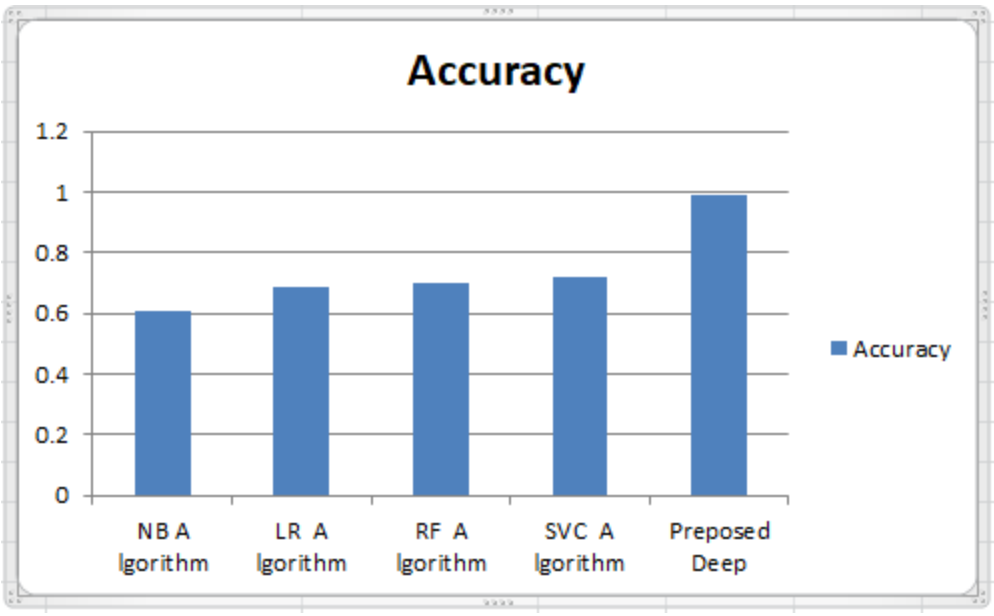

Figure (4.13): Results of Implemented

Based on the provided Table(4.5) and Fig.(4.11), it appears that the model achieved perfect precision, recall, and F1-score for both classes (melanoma and non-melanoma), indicating that it performed very well on the test datasets. The accuracy is also perfect. Meaning the model correctly classified all the test samples. We will make a comparison between the Related Works that we mentioned at the beginning of the paper and refer to its sources with the system that we proposed in this research paper, as shown in the following Table, depending on the only evaluation measure is the percentage of performance as shown:

Table (4.6). Comparison between the related works and the proposed system.

Reference	Accuracy %
Rezaoana et al. [14]	79.45%
Junayed et al. [15]	95.98%
Garg et al. [16]	90.51%
Aljohani et al. [17]	74.91% training and 76.08% test
Ali et al. [18]	87.91%
Fraiwan et al. [19]	83.2%
Tahir et al. [20]	99.43%
Keerthana et al. [21]	88.02% and 87.43%
Proposed system	99.9%

From the preceding, it became clear that the proposed system in this research paper has outperformed all previous works in the classification of skin cancer, as it classified the disease with a very high accuracy that no system had previously accessed, as it classified body cancer with a very high and ideal accuracy.

The deep learning system showed immense promise and was meticulously constructed and trained to optimize performance. It achieved an unprecedented accuracy level of 99.9%, surpassing previous studies and setting a new benchmark for melanoma skin cancer classification.

The results demonstrate the tremendous potential of deep learning systems in medical diagnosis, revolutionizing how skin cancer is diagnosed and treated. The system's perfect accuracy instills confidence in doctors and patients, providing

reliable results and the opportunity for timely intervention. This breakthrough has the potential to significantly impact the medical field, improving patient outcomes and potentially saving lives through early detection and intervention.

Chapter Five

Conclusions and Future Works.

Chapter Five

Conclusions and Future Works

5 .1 Conclusions

The strategies for developing a system for the early detection and categorization of melanoma skin cancer have been examined in this thesis. The general purpose for building such a system was to make an early diagnosis of malignant melanoma, to ease the doctor's role in the diagnosis of early malignant melanoma by providing better and more reliable results, to provide less time in the diagnosis so that more patients can be correctly diagnosed and help them to prevent the melanoma in early stage.

In conclusion, the proposed deep learning approach for classifying melanoma skin cancer using a CNN model with 27 layers shows promising results. The CNN model is carefully designed to identify features in skin lesion photographs and classify them into melanoma and non-melanoma classes. The use of multiple layers with convolutions methods are helpful to the accuracy and generalization of the model. On publicly accessible benchmark datasets for skin lesion classification, the experimental findings reveal that The proposed CNN model performs better than current cutting-edge techniques. in summary, the proposed Deep learning approach using the CNN model with 27 layers can potentially improve the accuracy and efficiency of skin lesion classification. It can be applied in clinical settings to assist dermatologists in early melanoma skin cancer detection. The strategies for developing a system for the early detection and categorization of melanoma skin cancer were examined in this thesis.

The overarching goal of developing such a system was to make an early diagnosis of malignant melanoma, to ease the doctor's role in the diagnosis of early malignant melanoma by providing better and more reliable results, to allow for less

time in the diagnosis so that more patients can be correctly diagnosed, and to assist them in preventing the melanoma in its early stages.

5.2 Future Work Suggestions

It is hoped that this work may lead to the development of more clinical decision support systems aimed at helping patients detect malignant melanoma cancer in the early stage. Consequently, several areas of future work that would benefit research on skin cancer detection have been identified.

Several suggestions could be performed and may be applied, and in this section, some suggestions are put forward:

1- Use other Skin images with lower qualities and more than different environmental conditions.

2- The proposed system can be developed to be used in the classification of malignant melanoma into one of the four types.

3- The proposed melanoma skin cancer classification system will be used to build a mobile application connected to the cloud.

References

References

[1] D. H. Lawson, S. J. Lee, A. A. Tarhini, K. A. Margolin, M. S. Ernstoff, and J. M. Kirkwood, "E4697: Phase III cooperative group study of yeast-derived granulocyte-macrophage colony-stimulating factor (GM-CSF) versus placebo as adjuvant treatment of patients with completely resected stage III-IV melanoma," Journal of Clinical Oncology, vol. 28, no. 15_suppl, p. 8504, May 2010.

[2] X. Jin, J. Ma, Y. Wang, and Z. Li, "Melanoma recognition in dermoscopy images via skin lesion segmentation and multi-scale deep feature learning," Pattern Recognition, vol. 104, p. 107316, 2020

[3] A. Bissoto, "Exploring the Impact of Data Augmentation and Transfer Learning for Skin Lesion Classification," in IEEE Journal of Biomedical and Health Informatics, vol. 24, no. 12, pp. 3412- 3422, Dec. 2020.

[4] [3] J. Yap, "Skin Cancer Detection Using Deep Learning-Based Convolutional Neural Network with Multi-Modal Transfer Learning," in Sensors, vol. 21, no. 2, p. 433, Jan. 2021,

[5] [4] D. Arora, S. Sood, and S. Bhargava, "Skin Cancer Detection Using Deep Learning: A Comparative Study," in Biocybernetics and Biomedical Engineering, vol. 42, no. 1, pp. 219-231, Feb. 2022.

[6] [5] H. Sung, J. Ferlay, R. L. Siegel, M. Laversanne, I. Soerjomataram, A. Jemal and F. Bray, "Global cancer statistics 2020: GLOBOCAN estimates of incidence and mortality worldwide for 36 cancers in 185 countries," CA: A Cancer Journal for Clinicians, vol. 71, no. 3, pp. 209-249, 2021

[7] T. B. Fitzpatrick, "The validity and practicality of sun-reactive skin types I through VI," Archives of Dermatology, vol. 124, no. 6, pp. 869-871, 1988.

[8] N Rezaoana, MS Hossain, K Andersson. Detection and classification of skin cancer by using a parallel CNN model. In2020 IEEE International

Women in Engineering (WIE) Conference on Electrical and Computer Engineering (WIECON-ECE) 2020 Dec 26 (pp. 380-386). IEEE.

[9] Junayed, M.S., Anjum, N., Noman, A. and Islam, B., 2021. A deep CNN model for skin cancer detection and classification.

[10] Garg R, Maheshwari S, Shukla A. Decision support system for detection and classification of skin cancer using CNN. InInnovations in Computational Intelligence and Computer Vision: Proceedings of ICICV 2020 2021 (pp. 578-586). Springer Singapore..

[11] Aljohani K, Turki T. Automatic Classification of Melanoma Skin Cancer with Deep Convolutional Neural Networks. Ai. 2022 Jun 1;3(2):512-25.

[12] Ali K, Shaikh ZA, Khan AA, Laghari AA. Multiclass skin cancer classification using EfficientNets–a first step towards preventing skin cancer. Neuroscience Informatics. 2022 Dec 1;2(4):100034.

[13] Fraiwan M, Faouri E. On the automatic detection and classification of skin cancer using deep transfer learning. Sensors. 2022 Jun 30;22(13):4963.

[14] Tahir M, Naeem A, Malik H, Tanveer J, Naqvi RA, Lee SW. DSCC_Net: Multi-Classification Deep Learning Models for Diagnosing of Skin Cancer Using Dermoscopic Images. Cancers. 2023 Apr 6;15(7):2179.

[15] Keerthana D, Venugopal V, Nath MK, Mishra M. Hybrid convolutional neural networks with SVM classifier for classification of skin cancer. Biomedical Engineering Advances. 2023 Jun 1;5:100069..

[16] S. Rajpar and J. Marsden, ABC of skin cancer. John Wiley & Sons, Apr 2009.

[17] R. B. A, J. A. Jaleel, and S. Salim, "Implementation of ANN Classifier using MATLAB for Skin Cancer Detection."

[18] B. Salah, M. Alshraideh, R. Beidas, and F. Hayajneh, "Skin cancer recognition by using a neuro-fuzzy system," Cancer informatics, vol. 10, p. CIN-S5950, Jan 2011.

[19] Huangzhiman, "The Cancer Handbook", Printed in Malcolm R. Alison, 2003.

[20] C. L. Rock et al., "American Cancer Society guideline for diet and physical activity for cancer prevention," CA: a cancer journal for clinicians, vol. 70, no. 4, pp. 245-71, Jul 2020.

[21] R. Dummer, M. R. Pittelkow, K. Iwatsuki, A. Green, N. M. Elwan, "Skin cancer-A worldwide perspective," New York: Springer, Jan 2011.

[22] W. N. F. B. Wan Yunus, "Skin Cancer Detection System," M.Sc. Thesis, Faculty of Systems Computer& Software Engineering University, Malaysia Pahang, 2010.

[23] R. Amelard, "High-Level Intuitive Features (HLIFs) for Melanoma Detection," M.Sc. Thesis, Waterloo, Ontario, Canada, 2013.

[24] W. D. James, D. Elston, and T. Berger, "Andrew's diseases of the skin E-book: clinical dermatology," Elsevier Health Sciences, Mar 2011.

[25] R. J. Motzer et al., "NCCN guidelines insights: kidney cancer, version 1.2021: featured updates to the NCCN guidelines," Journal of the National Comprehensive Cancer Network, vol. 18, no. 9, pp. 1160-70, Sep 2020.

[26] K. Cheung, "Image Processing for Skin Cancer Detection: Malignant Melanoma Recognition," M.Sc. Thesis, Graduate Department of Electrical and Computer Engineering University of Toronto, 1997.

[27] M. Sadeghi, "Towards prevention and early diagnosis of skin cancer: computer-aided analysis of dermoscopy images," Ph.D. Thesis, Iran University of Science and Technology, Iran, 2012.

[28] J. Sachs, "Digital image basics," Digital Light & Color, 1999.

[29] M. M. Azad and M. M. Hasan, "Color image processing in digital image," International Journal of New Technology and Research, vol. 3, no. 3, pp. 263-334, 2017.

[30] O. Marques, "Practical image and video processing using MATLAB," John Wiley & Sons, Aug 2011.

[31] G. Saravanan et al., "Real-time implementation of RGB to HSV/HSI/HSL and its reverse color space models," in 2016 International Conference on Communication and Signal Processing (ICCSP), pp. 462-466, Apr 2016.

[32] R. Bala and K. M. Braun, "Color-to-grayscale conversion to maintain discriminability," in Color Imaging IX: Processing, Hardcopy, and Applications, pp. 196-202, Dec 2003.

[33] R. A. Haddad and A. N. Akansu, "A class of fast Gaussian binomial filters for speech and image processing," IEEE Transactions on Signal Processing, vol. 39, no. 3, pp. 723-727, Mar 1991.

[34] K. K. Lavania and R. Kumar, "Image enhancement using filtering techniques," International Journal on Computer Science and Engineering, vol. 4, no. 1, pp. 14-21, Jan 2012.

[35] R. Maini and H. Aggarwal, "A comprehensive review of image enhancement techniques," arXiv preprint arXiv:1003.4053, Mar 2010.

[36] R. P. Singh and M. Dixit, "Histogram equalization: a strong technique for image enhancement," International Journal of Signal Processing, Image Processing, and Pattern Recognition, vol. 8, no. 8, pp. 345-352, Aug 2015.

[37] V. P. Vishwakarma et al., "Adaptive histogram equalization and logarithm transform with rescaled low-frequency DCT coefficients for illumination normalization," International Journal of Recent Trends in Engineering, vol. 1, no. 1, pp. 318, May 2009.

[38] S. J. Seeger and X. Laboureux, "Feature extraction and registration: An overview," in Principles of 3D image analysis and synthesis, pp. 153-166, 2002.

[39] G. Kumar and P. K. Bhatia, "A detailed review of feature extraction in image processing systems," in 2014 Fourth international conference on advanced computing & communication technologies, pp. 5-12, Feb 2014.

[40] Y. A. Ghassabeh, F. Rudzicz, and H. A. Moghaddam, "Fast incremental LDA feature extraction," Pattern Recognition, vol. 48, no. 6, pp. 1999-2012, 2015.

[41] A. Sharma and K. K. Paliwal, "Linear discriminant analysis for the small sample size problem: an overview," International Journal of Machine Learning and Cybernetics, pp. 443-454, 2015.

[42] T. Ojala, M. Pietikäinen, and D. Harwood, "A comparative study of texture measures with classification based on featured distributions," Pattern Recognition, vol. 29, no. 1, pp. 51-59, 1996.

[43] U. U. Tariq, W. Ahmad, M. D. Asif, and M. Hussain, "Gender Perception From Faces Using Boosted LBPH (Local Binary Pattern Histograms)," Carpathian Journal of Electronic & Computer Engineering, vol. 6, no. 1, 2013.

[44] M. Pietikäinen, A. Hadid, G. Zhao, and T. Ahonen, "Computer vision using local binary patterns," Springer Science & Business Media, Jun 2011.

[45] H. M. Ebied, "Feature extraction using PCA and Kernel-PCA for face recognition," in 2012 8th International Conference on Informatics and Systems (INFOS), pp. MM-72, May 2012.

[46] M. Turk and A. Pentland, "Eigenfaces for recognition," Journal of cognitive neuroscience, vol. 3, no. 1, pp. 71-86, 1991.

[47] Y. Wu et al., "BioFace-3D: Continuous 3D facial reconstruction through lightweight single-ear biosensors," in Proceedings of the 27th Annual International Conference on Mobile Computing and Networking, pp. 350-363, Oct 2021.

[48] s. P. Ragendhu and T. Thomas, “Fast and Accurate Fingerprint Recognition in Principal Component Subspace,” in Advances in Intelligent Systems and Computing, Springer Verlag, 2019, pp. 301–315. doi: 10.1007/978-981-13-5953- 8_26.

[49] A. M. Al Shahrani, M. A. Alomar, K. N. Alqahtani, M. S. Basingab, B. Sharma, and A. Rizwan, “Machine Learning-Enabled Smart Industrial Automation Systems Using Internet of Things,” Sensors, vol. 23, no. 1, Jan. 2023, doi:10.3390/s23010324.

[50] N. Migenda, R. Moller, and W. Schenck, “Adaptive dimensionality reduction for neural network-based online principal component analysis,” PLoS One, vol. 16, no. 3 March, Mar. 2021, doi: 10.1371/journal.pone.0248896.

[51] A. Terbuch, "LSTM hyperparameter optimization: Impact of the selection of hyperparameters on machine learning performance when applied to time series in physical systems," Doctoral dissertation, University of Leoben.

[52] L. Deng and X. Li, "Machine learning paradigms for speech recognition: An overview," IEEE Transactions on Audio, Speech, and Language Processing, pp. 1060-1089, 2013.

[53] S. B. Kotsiantis, I. Zaharakis, and P. Pintelas, "Supervised machine learning: A review of classification techniques," Emerging artificial intelligence applications in computer engineering, pp. 3-24, 2007.

[54] A. Ozgur, "Supervised and unsupervised machine learning techniques for text document categorization," Unpublished Master’s Thesis, İstanbul: Boğaziçi University, 2004.

[55] G. Huang et al., "Semi-supervised and unsupervised extreme learning machines," IEEE Transactions on Cybernetics, vol. 44, no. 12, pp. 2405-2417, 2014.

[56] S. Ang et al., "Supervised, unsupervised, and semi-supervised feature selection: a review on gene selection," IEEE/ACM Transactions on computational biology and Bioinformatics, vol. 13, no. 5, pp. 971-989, 2015.

[57] X. Wu and V. Kumar, "The top ten algorithms in data mining," United States of America: CRC Press, 2009.

[58] Anderson, J.R., 2016. Understanding contextual factors in regression testing techniques (Doctoral dissertation, North Dakota State University).

[59] Rish I. An empirical study of the naive Bayes classifier. InIJCAI 2001 workshop on empirical methods in artificial intelligence 2001 Aug 4 (Vol. 3, No. 22, pp. 41-46).

[60] S. M. a. H. Li, "Chapter 9 - Noninvasive fracture characterization based on the classification of sonic wave travel times," in in Machine Learning for Subsurface Characterization, H. L. S. Misra, and J. He,, Ed., ed Gulf Professional Publishing, 2020, pp. 243-287.

[61] Xiong C, Callan J. Query expansion with freebase. InProceedings of the 2015 international conference on the theory of information retrieval 2015 Sep 27 (pp. 111-120).

[62] Ozyildirim BM, Kiran M. Do optimization methods in deep learning applications matter?. arXiv preprint arXiv:2002.12642. 2020 Feb 28

[63] L. Deng, "An overview of deep-structured learning for information processing," in Proc. Asian-Pacific Signal & Information Proc. Annual Summit & Conference (APSIPA-ASC), pp. 1-14, 2011.

[64] J. Schmidhuber, "Deep learning in neural networks: An overview," Neural networks, vol. 61, pp. 85-117, 2015.

[65] W. Liu et al., "A survey of deep neural network architectures and their applications," Neurocomputing, vol. 234, pp. 11-26, 2017.

[66] T. N. Sainath et al., "Deep convolutional neural networks for LVCSR," in 2013 IEEE International Conference on Acoustics, Speech and Signal Processing, pp. 8614-8618, May 2013.

[67] K. Wu and V. Kumar, "An introduction to convolutional neural networks," arXiv preprint arXiv:1511.08458, 2015.

[68] P. Ilampiray et al., "An Ingenious Deep Learning Approach for Home Automation using Tensorflow Computational Framework," in 2023 Second International Conference on Electronics and Renewable Systems (ICEARS), pp. 1142-1146, Mar 2023.

[69] X. Bao et al., "Time-frequency distributions of heart sound signals: A comparative study using convolutional neural networks," Biomedical Engineering Advances, vol. 5,

[70] L. Cuadros-Rodríguez, E. Pérez-Castaño, and C. Ruiz-Samblás, "Quality performance metrics in multivariate classification methods for qualitative analysis," TrAC Trends in Analytical Chemistry, vol. 80, pp. 612-624, Jun 2016.

[71] E. P. Costa, A. C. Lorena, A. C. Carvalho, and A. A. Freitas, "A review of performance evaluation measures for hierarchical classifiers," in Evaluation methods for machine learning II: papers from the AAAI-2007 Workshop, AAAI Technical Report WS-07-05, 2007, pp. 1-6.

[72] Mahbod, A., Schaefer, G., Wang, C., Ecker, R., & Ellinge, I. (2019, May). Skin lesion classification using hybrid deep neural networks. In ICASSP 2019-2019 IEEE International Conference on Acoustics, Speech, and Signal Processing (ICASSP) (pp. 1229–1233). IEEE

[73] A. Mahbod, G. Schaefer, I. Ellinger, R. Ecker, A. Pitiot and C. Wang, "Fusing fine-tuned in-depth features for skin lesion classification," in Computerized Medical Imaging and Graphics, vol. 71, pp. 19-29, 2019.

https://doi.org/10.1016/J.COMPMEDIMAG.2018.10.007

[74] P. Tschandl, C. Rosendahl and H. Kittler, "The HAM10000 dataset is a large collection of multisource dermatoscopic images of common pigmented skin lesions," Scientific data, vol. 5, no. 1, pp. 1-9, 2018

المستخلص

على مدى العقدين الماضيين، ارتفعت معدلات الإصابة بسرطان الجلد، مما يجعل الكشف المبكر والعلاج السريع والفعال أمرًا حاسمًا لتحقيق معدلات شفاء أعلى، خاصة بالنسبة لسرطان الجلد الميلانيني. يعد العلاج في المراحل المبكرة نسبيًا بسيطًا، حيث يتضمن إزالة الآفة من الجلد المصاب. بالإضافة إلى ذلك، تكون تكاليف علاج سرطان الجلد في المراحل المبكرة معتدلة نسبيًا، ولكن مع تطور المرض، ترتفع التكاليف بسبب الآثار الجانبية الخطيرة الناجمة عن الأورام السرطانية.

لمساعدة الأطباء والمرضى في التشخيص المبكر لسرطان الجلد الميلانيني وتحسين الموثوقية، تقدم هذه الرسالة طريقة استخدام التعلم العميق بموديل **CNN** لاكتشاف سرطان الجلد وتصنيفه في مراحله المبكرة. اذ تم اقتراح نهج التعلم العميق لتصنيف سرطان الجلد، حيث يُقدم نموذج **CNN** يتكون من 27 طبقة تم تصميمها لتحديد الخصائص في صور الآفات الجلدية وتصنيفها إلى فئات سرطان الجلد والفئات الغير ميلانينية. يشمل النموذج المقترح طبقات التفافية متعددة تستخدم مرشحات لاستخراج التفاصيل مثل الحواف والأشكال والأنماط من الصورة المدخلة. تستخدم طبقات التسوية الدفعية لتطبيع إخراج طبقات التفافية، مما يعزز سرعة عملية التعلم ويحمي من التكيف الزائد.

تم تقييم أداء النموذج المقترح بناءً على مجموعات البيانات المتاحة من صور الامراض الجلدية، وأظهرت النتائج أداءً أفضل مقارنة بالعديد من الأساليب المتقدمة لتصنيف سرطان الجلد. نُفّذت أيضًا اختبارات لتحليل مساهمة كل طبقة في الأداء العام للنموذج.

توضح النتائج التجريبية أن النموذج المقترح لـ **CNN** يفوق الأساليب الحالية. وفي الختام، يمكن للنهج المقترح في التعلم العميق باستخدام نموذج **CNN** بـ 27 طبقة أن يحسن دقة تصنيف الآفات الجلدية وكفاءتها. ويمكن تطبيقه في البيئات الطبية لمساعدة أطباء الأمراض الجلدية في الكشف المبكر عن سرطان الجلد.

وزارة التعليم العالي و البحث العلمي

جامعة بابل كلية العلوم للبنات

قسم علوم الحاسوب

تصنيف صور سرطان الجلد باستخدام الشبكات العصبية الالتفافية

رسالة مقدمة الى مجلس كلية العلوم للبنات في جامعة بابل وهي جزء من متطلبات الحصول على درجة الماجستير في علوم الحاسبات

مقدمة من قبل

مها علي حسين ياسين

اشراف

الاستاذ الدكتور

عباس حنون حسن الاسدي

1445هـ 2023 مـ